Aus der Klinik und Poliklinik für Anästhesiologie, Intensivmedizin,
Notfallmedizin und Schmerztherapie

Effect of Tjap1 knock-down on blood-brain barrier properties under normal and hypoxic conditions

Inauguraldissertation
zur Erlangung der Doktorwürde der Medizinischen Fakultät
der
Julius-Maximilians-Universität Würzburg
vorgelegt von

Aili Sun

aus
Heilongjiang, China

Würzburg, März 2023

Referent bzw. Referentin: Priv.-Doz. Dr. rer. nat. Malgorzata Burek

Korreferent bzw. Korreferentin: Prof. Dr. rer. nat. Dr. med. Barbara Braunger

Dekan: Prof. Dr. med. Matthias Frosch

Tag der mündlichen Prüfung: 6. Dezember 2023

Die Promovendin ist Ärztin

Table of contents

1. Introduction

1.1 Stroke

Ischemic stroke is a life-threatening neurological disorder caused by a lack of blood supply to the brain and a loss of vascular integrity, leading to neuronal cell damage in the brain parenchyma [1, 2]. Stroke is the second leading cause of death worldwide, affecting over 15 million people each year [3, 4]. Stroke causes not only primary damage but also secondary brain damage caused by the mass effect, glucose and oxygen starvation, coagulation problems, oxidative stress, excitotoxicity, etc. [5, 6]. Inflammation and subsequent brain damage result from leakage of the blood-brain barrier (BBB), which is dysregulated after brain disease and injury [7].

1.2 Blood-brain barrier

The BBB serves as an interface between the circulation and brain tissue [8]. Cell-cell interactions within the neurovascular unit (NVU) maintain the stability of the BBB. The NVU is a structural component that includes endothelial cells, pericytes, astrocytes, microglia, and neurons [8-12]. The BBB is formed primarily by a single layer of endothelial cells that form the vessel wall and exhibit specific biological features. BBB prevents free cellular bypasses through the capillary wall. Endothelial cells of the central nervous system (CNS) have specific features such as highly specialized cell-cell junctions including tight junctions (TJs) and adherent junctions (AJs) [13]. Brain microvascular endothelial cells express specialized transport proteins to control the dynamic inflow and outflow of substances and display a very low rate of transcytosis [14, 15].

1.3 Factors associated with the blood-brain barrier

BBB homeostasis is disrupted by changes in its function and structure. Formation, alteration in expression and distribution of TJ and AJ proteins, followed by the changes of the local microenvironment, transporter system, enzymes, and extracellular matrix (ECM), result in the passage of harmful serum components and immune cells through the BBB, disturbing the CNS homeostasis and causing damage to the brain parenchyma.

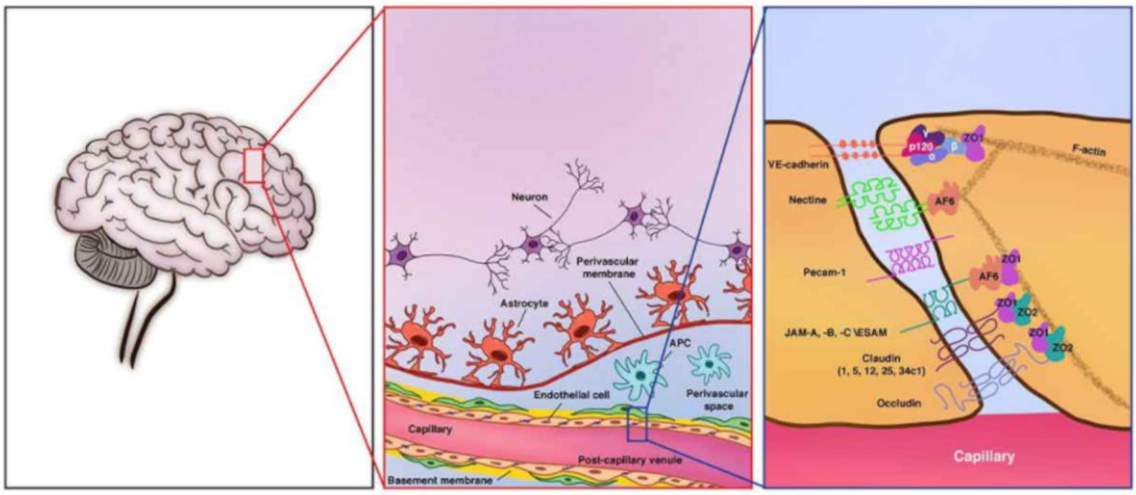

Figure 1. Structure of the blood-brain barrier. The image of the brain with magnifications shown on the right. The neurovascular unit is formed by endothelial cells of the brain capillaries, basal membrane, astrocytes, pericytes and neurons. As shown on the right, endothelial cells form tight junctions and adherens junctions that are connected to the actin cytoskeleton. Image modified from Scalise et al. 2021 [16] (open access).

1.3.1 TJ protein composition and role

Brain microvascular endothelial cells exhibit high transendothelial electrical resistance (TEER) due to the presence of TJs and AJs that prevent water and solutes from freely passing the BBB [17]. The transmembrane proteins claudins, tricellulin, occludin, junctional adhesion molecules (JAMs), and zonula occludens (ZO) proteins are mainly involved in TJs and AJs [18, 19]. Transmembrane TJs proteins have been shown to be essential to maintain the functional integrity of the BBB. Claudins are a family of proteins with a molecular weight of 20–24 kDa. Brain endothelial cells mainly express claudin-1, -3, -5 and -12, while the presence of other claudins at the BBB has recently been demonstrated [20]. Claudins limit the transport of smaller molecules across the BBB [21, 22]. In addition, tricellulin is considered to play a function in restricting the paracellular transport of larger molecules [22, 23]. JAMs are members of the immunoglobulin subfamily with a molecular weight of almost 40 kDa and are involved in the modulation of the paracellular permeability of the BBB [24, 25]. ZO-1, ZO-2 and ZO-3 are important scaffold proteins [26], [27]. Among them, ZO-1 is critical for the stability and functionality of TJs [28-30] such that it binds transmembrane TJ proteins

to the actin cytoskeleton [31, 32]. Tjap1 (other name Protein Incorporated Later Into Tight Junctions, Pilt), a protein associated with tight junctions, is located to the Golgi apparatus and may be involved in vesicle transport. The protein is incorporated into TJs at a late stage of junction formation [33, 34].

1.3.2 AJs protein composition and role

AJs, which are adhesive structures but not as tight as TJs, support TJs by creating strong adhesive bonds between adjacent cells [35]. AJs mediate cell signaling, transcriptional and actin cytoskeleton modulation in addition to stabilizing intercellular adhesion [36, 37]. The functions of AJs and TJs is linked [38-40]. The vascular endothelial adhesion protein, VE-cadherin, which is important for TJ formation and stability, is applied to establish essential cell junctions [8, 41]. TJs are affected by claudins and JAMs, while AJs are influenced by cadherins and nectins. Previous studies revealed that nectins first form cell-cell adhesion, where cadherins are recruited to form AJs. Thereafter, claudins and JAMs are recruited to the apical side of AJs to form TJs [42-44].

1.3.3 ABC transporter proteins

ABC transporter proteins contain 48 members and are divided into seven sub-families based on their structural homology. P-glycoprotein (P-gp, Abcb1), multidrug resistance-associated proteins (Mrp), and breast cancer resistance protein (Bcrp, Abcg2) are the most notable BBB transporters [7, 45]. P-gp prevents a variety of lipid-soluble chemicals from accumulating in the brain parenchyma by transporting them away from the CNS and brain capillary endothelium [46, 47]. There are 13 components that constitute Mrp family, including truncated proteins, surface receptors, and ion channels. The endoplasmic reticulum produces P-gp, which has a molecular weight of 170 kDa, and the Golgi apparatus glycosylates it to preserve it from dissolving [48, 49]. Mrp1 (Abcc1) is a potent efflux transporter. It plays a critical role in inflammatory mechanisms by promoting the transfer of the inflammatory mediators, leukotriene C4 and prostaglandin E2, the efflux of various internal and external metabolites, and being involved in defence against oxidative stress [50, 51].

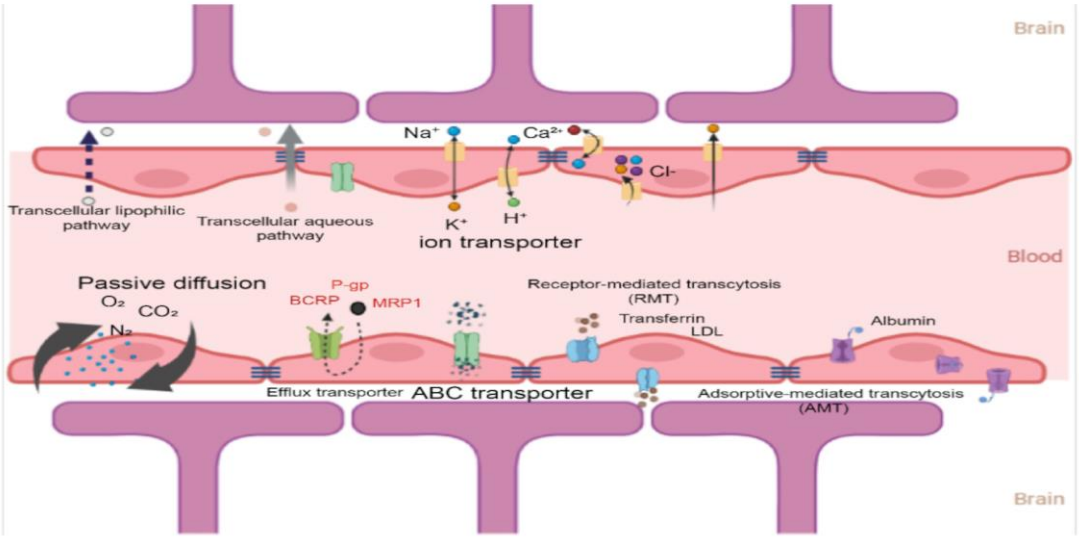

Figure 2. **Schematic representation of mechanisms for crossing the blood-brain barrier.** Gaseous molecules (O_2, CO_2, N_2) can pass through the BBB by passive diffusion. Efflux pumps (ABC transporter) protect the brain by pumping out the molecules. Receptor-mediated transcytosis and carrier-mediated transport provide the brain with nutrients such as glucose and amino acids. Image modified from Zhao et al. 2022 [52] (open access).

1.3.4 Inflammatory factors and TJ proteins

There is accumulating evidence that the impairment of paracellular and transcellular transport pathways in stroke and traumatic brain injury (TBI) are primarily related to oxidative stress and neuroinflammation. First, in the context of oxygen/glucose deprivation (OGD), Brain endothelial cells upregulate cell adhesion molecules, including Icam-1 and Vcam-1, to trigger local inflammatory responses and release pro-inflammatory regulators [53]. Second, the increased permeability of the BBB is triggered by phosphorylation of TJ proteins, which is promoted by inflammatory mediators generated after ischemic brain injury. ZO-1 is significantly phosphorylated on the tyrosine, threonine, and serine residues in cultured brain ECs with cytokines or chemokines such as tumor necrosis factor (TNF)-α, Il-6, and monocyte chemotactic protein 1 (Mcp1)/Ccl2 [54-56]. After monocytes were co-cultured with ECs, Rho/Rock were activated. As a result, occludin and claudin-5 were phosphorylated on serine and tyrosine residues, which increased the amount of monocytes migrating across the BBB [57]. Numerous studies have been performed on the dynamic behaviour of TJ proteins of epithelial cells in peripheral organs [58]. TJ flexibility and barrier properties are

significantly regulated by the internalization of TJ proteins into cell membranes, and subsequent transport, recycling and destruction [58].

1.4 Effect of OGD on blood-brain barrier function

On the one hand, reduced glucose and oxygen supply has been observed in certain regions of the brain after stroke or trauma, resulting in significantly decreased ATP and ion imbalance, ECM degradation [59], actin contraction, increased cytoskeletal tension, and modified endothelial cell morphology. On the other hand, the expression of TJ-related proteins such as occludin, claudin-5, and ZO-1 is regulated, and BBB permeability is increased [60-62]. In addition, immune cells invade the NVU and generate an inflammatory response within the brain [63]. After a stroke and / or traumatic event, the release of inflammatory cytokines can result in the degradation of cerebrovascular junctional proteins [64, 65]. This leads to an increase in the paracellular permeability of the BBB. We use the OGD approach to simulate the *in vitro* post-stroke or trauma environment for 4h followed by 2h reoxygenation. This method, with some modifications, has previously been shown to be a reliable *in vitro* method that mimics stroke conditions. Numerous studies have shown that brain endothelial cell lines cEND and cerebEND cell lines exhibit altered BBB properties after 4h of OGD treatment, such as reduced TEER, increased permeability and altered expression of tight junction proteins, transport proteins, and matrix metalloproteinases [66].

1.5 cEND and cerebEND

We used the cEND and cerebEND mouse immortalized cerebral and cerebellar endothelial cell lines, respectively [67, 68]. As shown in previous work, these cell lines express important junctional proteins including claudin-5, occludin and VE-cadherin. Both cell lines expressed BBB-specific markers and formed a stable barrier *in vitro* as confirmed by TEER and permeability measurement. Furthermore, after exposure to low serum content media, cEND and cerebEND cell lines showed increased cell layer density, decreased macromolecule permeability, and changes in TJ protein expression [69-71]. TNF-α treatment was used to assess inflammation-mediated changes in cEND and cerebEND which manifested in impaired barrier function and the altered levels of TJ proteins. The effect was more pronounced in the cerebEND cell line than in cEND.

This shows that various immortalized endothelial cell lines from different brain areas have different barrier characteristics. Thus, cEND and cerebEND cell lines can be considered as suitable *in vitro* models to study BBB properties [72-79].

1.6 Aim of the work

Previous studies have shown that stroke and *in vitro* OGD treatment resulted in compromised BBB integrity and significantly increased expression of microRNA-212/132. Three genes encoding proteins associated with BBB integrity, including Tjap1, claudin-1 and Jam-3 have been identified as direct targets of microRNA-212/132 [80]. To date, little is known about the cellular function of Tjap1 at the BBB. Therefore, the aim of this dissertation was to elucidate the role of Tjap1 in brain microvascular endothelial cells. For this purpose we generated Tjap1 knock-down (Tjap1 KD) cEND and cerebEND cell lines and examined the effects of Tjap1 KD on barrier properties, migration and proliferation rate, angiogenic potential and expression of BBB and endothelial cell markers.

2. Materials and methods

2.1 Materials

2.1.1 Chemicals

Table 1: Abbreviations and manufacturers of applied chemicals

Chemical	Manufacturer
High Capacity cDNA Reverse Transcriptase Kit	Thermo Fisher Scientific
Dextrose [D(+)-Glucose-Monohydrat] Isopropanol Sodium fluoride (NaF)	Merck – Life Science
Chloroform Enhanced chemiluminescence solution (ECL)	Roche Diagnostics
Agarose Albumin from bovine serum (BSA) Ammonium persulfate (APS) Bromophenol Blue CHAPS 4',6-diamidino-2-phenylindole (DAPI) Diethylpyrocarbonate (DEPC) Dextran (70 kDa) Dimethysulfoxide (DMSO) Dulbecco's Phosphate Buffered Saline (PBS) Ethylenediaminetetraacetic acid (EDTA) Evans Blue Glutaraldehyde Glycine Guanidine hydrochloride HEPES Proteinase K Sodium dodecyl sulphate (SDS) Tetramethylethylenediamine (TEMED)	Sigma-Aldrich

Thiourea Tris hydroxymethyl aminomethane (Tris) Triton™ X-100	
Pierce BCA Protein Assay Kit	Thermo Fisher Scientific, # 23225
NucleoSpin® miRNA Kit	Macherey Nagel, #740971.50
ECM Cell Adhesion Array (Colorimetric)	Merck – Life Science, # ECM540

2.1.2 Consumables

Table 2: Consumables

Company	**Consumables**
Thermo Fisher Scientific	24 well plate Nuclon Surface
Greiner Bio One	24 well Trans-well plate (ThinCert, pore size 0,4µm) 12 well plate Nuclon Surface 6 well plate Nuclon Surface
Thermo Fisher Scientific	96 well plate 48 well plate 12 well plate 6 well plate
Sarstedt AG & Co	Biosphere® Filter Tips, sterile 0,5-20µl Biosphere® Filter Tips, sterile 2-100µl Biosphere® Filter Tips, sterile 100-1000µl
Ibidi GmbH	Culture-Insert 2 well in µ-Dish 35 mm
Thermo Fisher Scientific	MicroAmp™ Optical 96 well reaction plate Thermo MicroAmp™ Optical Adhesive Film Nalgene Cryogenic Vials

2.1.3 Antibodies (Abs)

Table 3: Suppliers and dilution ratio of primary Abs for WB

Primary antibody	Company	Catalog number	Concentration
Rabbit anti-Tjap1	Abcam	Ab80444	1:1000
Mouse anti-claudin-1	Santa Cruz Biotechnology	Sc-166338	1:200
Mouse anti-claudin-5	Thermo Fisher Scientific	35-2500	1:500
Rabbit anti-claudin-12	IBL-International	JP18801	1:100
Rabbit anti-Jam-C	Merck – Life Science	ABT31	1:2000
Rabbit anti-VCAM-1	Cell Signaling Technology	Ab14694s	1:800
Rabbit anti-ZO-1	Thermo Fisher Scientific	61-7300	1:500
Human anti-VE-cadherin	Santa Cruz Biotechnology	Sc-6458	1:200
Mouse anti-Pgp	Enzo Life Sciences	ALX-801-002-C100	1:20
Rabbit anti-Mrp-1	Sigma-Aldrich	SAB2100010-Lot: QC13897	1:500
Rabbit anti-TIMP-3	Abcam	Ab39184	1:100
Guinea pig anti-occludin	Acris GmbH	AP26410 PU-N	1:100
Rabbit anti-VEGF	Santa Cruz Biotechnology	Sc-507	1:100
ß-actin-Peroxidase	Sigma-Aldrich	A 3854	1:25000
Anti-Mouse IgG	Cell Signaling Technology	HRP-linked Antibody 7076s	1:3000
Anti-Rabbit IgG	Cell Signaling Technology	HRP-linked Antibody 7074s	1:3000

2.1.4 Probes real-time PCR

Table 4: Probes real-time PCR

Probe	Manufacturer and assay number
Actb	Thermo Fisher Scientific Mm 01205647_g1
Abcc1	Thermo Fisher Scientific Mm 00456156_m1
Abcb1a	Thermo Fisher Scientific Mm 00440761_m1
Ccl-2	Thermo Fisher Scientific Mm 00441242_m1
Ccl-5	Thermo Fisher Scientific Mm 01302427_m1
Ccl-7	Thermo Fisher Scientific Mm 00443113_m1
Csf-3	Thermo Fisher Scientific Mm 00438335_g1
Canx	Thermo Fisher Scientific Mm 00500330_m1
Claudin-1	Thermo Fisher Scientific Mm 00516701_m1
Claudin-5	Thermo Fisher Scientific Mm 00727012_s1
Claudin-12	Thermo Fisher Scientific Mm 01316511_m1
Cdh-5/VE-Cadherin	Thermo Fisher Scientific Mm 00486938_m1
occludin	Thermo Fisher Scientific Mm 00500912_m1
Tjap1	Thermo Fisher Scientific Mm 00503864_m1

Timp-3	Thermo Fisher Scientific Mm 00441826_m1
Vcam-1	Thermo Fisher Scientific Mm 01320970_m1
ZO-1 (Tjp-1)	Thermo Fisher Scientific Mm 00493699_m1
Jam-3	Thermo Fisher Scientific Mm 00499214_m1

2.1.5 Transfection reagents

Table 5: Transfection reagents

Company (catalogue number)	**Plasmid**
Santa Cruz Biotechnology Sc-152265-SH. Lot # L2414	Pilt shRNA plasmid(m）
Santa Cruz Biotechnology Sc-430015-HDR. Lot # E2915	Pcdh2 HDR plasmid(m)
Santa Cruz Biotechnology Lot #12921	CRISPR/Cas9 diluent DNase-free H_2O
Thermo Fisher Scientific # L3000015	Lipofectamine 3000 Transfection Kit
Thermo Fisher Scientific # 31985062	OPTI-MEM® I (1 X) Reduced Serum Medium

2.1.6 Experimental software and hardware

Table 6: Suppliers and application of software for experimental analysis

Software	**Company**	**Application**
EndNote X9	Thomson Reuters GmbH	References managing
Sigma plot 12.5	Systat Software GmbH	Statistical analysis
Fiji/Image J software	National Institute of Health, Bethesda, MD, USA	Image processing and Image analysis
FluorChem FC2	Alpha-InnoTech	WB image

MultiImage II		densitometric analysis
QuantStudio™ 7 Flex Real-Time PCR Software v1.7.1	Thermo Fisher Scientific	PCR amplification and analysis

Table 7: Suppliers and application of hardware for experiment performance

Hardware	Company	Application
Eppendorf Thermal mixer®	Eppendorf AG	Sample heating
Nanodrop ND 2000 spectrophotometer	Thermo Fisher Scientific	RNA concentration measurement
Applied Biosystems 2720 Thermal Cycler	Thermo Fisher Scientific,	cDNA transcription
QuantStudio™ 7 Flex Real-Time PCR System	Thermo Fisher Scientific,	RT-PCR amplification
FluorChem FC2 MultiImage II Hardware	Alpha-InnoTech,	WB image scanning
Infinite M200 PRO Multimode Micoplate Reader	Tecan Deutschland GmbH	Protein concentration measurement for WB
KEYENCE BZ-9000 fluorescence microscopy	KEYENCE Corporation	Image acquisition and processing

2.1.7 Buffers

Table 8: Buffers

Buffers	Ingredients
0.1% DEPC solution	1 ml DEPC 1000 ml PBS
Protein wash buffer	0.3 M guanidine hydrochloride 95% ethanol
Protein lysis buffer	8 M Urea 2 M Thiourea

	4% CHAPS 100 mM Tris-HCI (PH 8.5)
1% EBA solution	0.1 g Evans blue dye 10 ml 5% BSA/PBS
Hypertonic saline	10 g NaCl 10 ml distilled H2O
Fluorescein solution	5 mg Fluorescein Ringer-HEPES buffer: 8,8 g NaCl 0,387 g KCl 0,244 g CaCl2 0,0406 g MgCl2; 6H2O 0,504 g NaHCO3 1,19 g HEPES 0,504 g Glucose
ECL I	25 ml Tris 1M pH 8,8 5 ml Luminol 2,2 ml p-Coumaric-Acid Ad 250 ml Distilled Wasser
ECL II	25 ml Tris 1 M, pH 8,8 160 µl Hydrogen Peroxide Ad 250 ml Distilled Water
Running Buffer	50 ml 20 x NuPAGE® MES or MOPS SDS Running Buffer to 950 mL deionized water to prepare 1 x SDS
50 x Transfer Buffer	50 ml NuPAGE® Transfer Buffer (20x) 100 ml NuPAGE® Antioxidant 100 ml Methanol 849 ml Deionized Water

2.2 Methods

2.2.1 Cell culture

2.2.1.1 Cell Culture & Freezing

For the experiments, the endothelial cell lines cEND [68] and cerebEND [67] were generated from murine cerebrum and cerebellum and used as *in vitro* models of the BBB. In previous studies, these cells were separated according to the standard protocol and stored in nitrogen tanks [81]. After removal from liquid nitrogen, the cells were carefully thawed in a 37°C water bath (GFL Technology) and then placed in 25 cm^2 cell culture flasks (Greiner Bio-One), which were coated with 0.5% gelatin or Speed coating solution (PeloBiotech) for 15 minutes.

For cerebEND cells, 10% fetal calf serum (FCS, Merck-Sigma) and 1% penicillin/streptomycin were added to DMEM (Dulbecco's modified eagle media) (Sigma-Aldrich). Meanwhile, cEND cells were plated on 0.5% gelatin-coated flask in Endothelial Cell Medium (CellBiologics) and supplemented with Endothelial cell culture kit (content: VEGF, Heparin, EGF, ECGS, Hydrocortisone, L-glutamine, Antibiotic-Antimitotic, FCS) (CellBiologics). Both cell lines were grown in 37 °C, 95% humidity, and 5% CO_2 incubator (Thermo Fisher Scientific).

The cell culture medium was changed every two to three days. Depending on the growth conditions, the cells were split after reaching confluence. The splitting ratio of cell lines was 1:2 or 1:3. Normally, the old medium was removed first, and then the cells were washed twice with 20 ml PBS (phosphate buffered saline, Sigma-Aldrich). The cells were then treated with 2 ml of prewarmed trypsin solution (Stem Pro Cell Dissociation Reagent, Thermo Fisher Scientific), while observing cell dissociation to avoid over-trypsinization. Warm complete medium was added to stop the process. The cell suspension was then divided into two or three gelatin-coated 25 cm^2 cell culture flasks. Remaining trypsinized cells were centrifuged at 100 x g for 5 minutes at room temperature and the medium was discarded. Thereafter, 1 ml of freezing solution (80% cell culture medium, 10% FCS, and 10% DMSO) was added to the cell pellet, which was then stored at -80°C and later kept in liquid nitrogen.

2.2.1.2 Oxygen/Glucose Deprivation

Endothelial cells were maintained under normoxic conditions in Endothelial Cell Medium at 37°C, 5% CO_2, and 21% O_2. For OGD, cells were washed with PBS and were cultured for 4 hours in Endothelial Cell Medium without Glucose and FCS at 37°C, 5% CO_2, and 1% O_2 [81]. After this time, the medium was replaced with Endothelial Cell Medium containing 0.1% glucose and 1% FCS, and the cells were placed for 2 hours at 37°C, 5% CO_2, and 21% O_2 for re-oxygenation.

2.2.1.3 Establishment of the Knock-down cell lines

The gene silencer technique with plasmids expressing shRNA against Tjap1 was used to generate the knock-down (KD) cell lines. The cerebEND and cEND cell lines were transfected with Pilt shRNA plasmid (m) (Sc-152265-SH, Santa Cruz Biotechnology) or the control HDR plasmid (Sc-428717-HDR, Santa Cruz Biotechnology). Both plasmids contain a puromycin resistance gene. For transfection, 1.5 – 2.5 x 10^5 cells/well were seeded on 6-well plates (6-well-Nuclon surface tissue plates, Greiner Bio One), and the transfection was carried out after 24 hours with a cell density of 40% to 80%. According to the manufacturer's instructions, the cells were transfected with Lipofectamine 3000 (Thermo Fisher Scientific) and 1 µg of Pilt shRNA plasmid (Tjap KD cell line) or HDR plasmids (control cell line) for 24-72 hours. The culture medium containing puromycin (Puromycin dihydrochloride from Streptomyces alboniger, P8833-100MG, Sigma-Aldrich) was added for selection of transfected clones after 24 hours. After the transfected cells reached confluence, the success of transfection was evaluated using PCR and WB techniques.

2.2.2 MTT

Cell viability and cellular metabolic activity were determined using the 3-(4,5-dimethylthiazolyl-2)-2,5-diphenyltetrazolium bromide (MTT) assay (Sigma-Aldrich). Wild type, control, and Tjap1 KD cEND cells were seeded at 2.5 x 10^4 cells/well in flat-bottom 96 well plates. After 24 hours, 100 µl of MTT solution (1 mg/mL) in DMEM without phenol red was added to each well and incubated at 37 °C for 4 hours. Formazan crystals were solubilized in 100 µl of isopropanol for 15 minutes, and the absorbance at 570 and 630 nm was measured using a Tecan Microplate Reader (Tecan).

2.2.3 BrdU

The proliferation assay was performed according to the manufacturer's instructions using a 5′-bromo-2′-deoxyuridine (BrdU) Cell Proliferation Assay ELISA Kit (Merck). In a gelatin-coated 96 well plate, wild type, control, and Tjap1 KD cEND cells (5 x 10^3 cells) suspended in 200 µL culture medium were seeded. The BrdU Label solution was added after the cells had attached, and the cells were allowed to grow for 24 hours. The absorbance was measured with a spectrophotometric plate reader (Tecan) at 450 and 540 nm.

2.2.4 Quantitative real-time polymerase chain reaction (qPCR)

2.2.4.1 RNA Isolation

The cells were split, seeded, and grown to confluence in 6 well plates (6-well-Nuclon Surface tissue plates, Greiner Bio One). The NucleoSpin® miRNA Kit (Macherey Nagel) was used to isolate the ribonucleic acid (RNA). The cells were first washed with PBS after the culture medium was removed. A mixture of 350 µl of RA1 lysis buffer and 3.5 µl β-mercaptoethanol (Sigma-Aldrich) was added to each well. The lysate was scraped with a cell scraper and placed in a sterile 1.5 ml Eppendorf tube. The lysates were either processed immediately or frozen for storage at -80°C.

The sample was passed 10 times through a 1 ml syringe (Braun) for further lysis and then placed in the first NucleoSpin filter and centrifuged for 1 minute at 11,000 x g (Heraeus Megafuge 16R, Thermo Fisher Scientific). After washing, the RNA was eluted in 40 µl of RNase-free water. The RNA concentration was then measured with a spectrometer (NanoDrop 2000, Thermo Fisher Scientific). Usually a RNA concentration of 200–300 ng/µl was obtained. RNA was stored in a -80°C freezer for further use.

2.2.4.2 Reverse transcription - cDNA synthesis

By using High Capacity cDNA Reverse Transcription Kit (Thermo Fisher Scientific), which can reverse transcribe up to 2 µg of RNA in a single reaction, the acquired RNA was used to generate single-stranded complementary DNA (cDNA). In each reaction,

6.8 µl of the master mix were added to the 0.2 ml reaction tubes (Eppendorf AG) according to the manufacturer's instructions.

Master mix (per reaction)

2 µL	10 x RT Buffer
0.8 µL	25 x dRTP Mix(100 mM)
2 µL	10 x RT Random Primers
1 µL	Multiscribe Reverse Transcriptase
1 µL	RNA Inhibitor
X µL	Nuclease-free H_2O

X µL 1 µg Template RNA)- H_2O and RNA depending on the RNA concentration up to the final volume of 20 µl

The volume of RNA solution required for 1 µg RNA per reaction was calculated. To achieve a final volume of 20 µl per reaction, the RNA was diluted with the appropriate amount of RNAase-free. The cDNA was synthesized in the thermal cycler (Thermal Cycler 2720, Thermo Fisher Scientific) using the following program:

25°C	37°C	85°C	4°C
10 min	120 min	5min	∞

The cDNA was then used directly or was frozen for storage at -20°C.

2.2.4.3 Quantitative real-time PCR

Quantitative real-time PCR was used to amplify and quantify the samples as it allows quantification of the amount of amplified DNA while the reaction is taking place and eliminates the need for further analytical steps. TaqMan mRNA expression assays (Thermo Fisher Scientific) use gene specific probes and oligonucleotides labelled with a fluorescent reporter dye at the 5' end and a so-called quencher at the 3' end. The quencher almost completely inhibits the reporter dye signal. The 5'-nuclease activity of the Taq polymerase enzyme induces the destruction of the probe and the release of the dye through the amplification of the specific DNA sequence.

5 µl of TaqMan Universal PCR Master Mix (Thermo Fisher Scientific) along with 0.5 µl of the specific TaqMan probe (Thermo Fisher Scientific) and 2 µl of nuclease-free

water (Ambion) were pipetted into a 384 well plate (MicroAmp Otical 384 well reaction plate, Thermo Fisher Scientific). Then 2.5 µl of the cDNA diluted 1:10 with nuclease-free water were added. To ensure a high level of sensitivity, qPCR was run in triplicates. The same method was used for the endogenous control, which was calnexin (CanX) (Mm00500330_m1).

Reaction mix:

5	µL	FAST QPCR ROX MIX
0.5	µL	Taqman probe (20x)
2	µL	H_2O (nuclease-free)
2.5	µL	cDNA (1:10 in H_2O-DNase free)

The plate was then completely covered with a film (MicroAmp Optical Adhesive Film, Thermo Fisher Scientific), vortexed to mix, and span using a bench top centrifuge (Thermo Fisher Scientific) to ensure no residue of the reaction mixture was adhering to the sides of the wells or the film.

Real-time PCR was then performed on the prepared plate and a PCR device (QuantStudio™ 7 Flex Real-Time PCR System, Thermo Fisher Scientific) was used. Fifty cycles followed the initiation at 95°C for 10 minutes, each cycle running 15 seconds at 95°C and one minute at 60°C.

The gene expression was normalized to the expression of the endogenous control using a QuantStuiodio™ Real-Time PCR Software v1.7.1 (Thermo Fisher Scientific).

2.2.5 Western Blot

2.2.5.1 Protein preparation

The cells were split, plated in 6 well plates (6 well Greiner Bio One Nuclon Surface tissue plates), and grown for six to seven days to confluence. After discarding the medium, the cells were washed ice-cold PBS twice. Protease inhibitor Cocktail (Roche) was added to the protein lysis buffer as described in Table 8. After a few minutes on ice, the cells were scraped out of the wells with a cell scraper (Sarstedt), and then transferred into prepared Eppendorf tubes. The samples were then used immediately for experiments or frozen at -80°C for further use.

2.2.5.2 Protein quantity determination

Frozen samples were slowly thawed on ice. Samples were processed in an ultrasound device (Bandelin electronic GmbH & Co. KG), for 0.5 s/3.0 s x 5 times. The amount of protein was then calculated from the supernatant, which was centrifuged at 11,000 x g for 1 minute at 4°C.

Pierce BCA Protein Assay Kit (Thermo Fischer Scientific) was used to quantify protein content by using bicinchoninic acid methods. Bovine serum albumin (BSA, Sigma-Aldrich) was first diluted in a standard dilution series from a concentration of 2000 µg/ml to 25 µg/ml according to the recommended protocol. A 96 well plate (Thermo Fisher Scientific) was used for the measurement, while the other wells were each filled with 22 µl of distilled water and 3 µl of the test samples. The BCA reaction solution (Reagent A: Reagent B 50:1) was then added to each well at a ratio of 200 µl. After 30 minutes of incubation at 37°C and cooling to the RT, the absorbance was measured at 560 nm in the microplate reader (Tecan). The protein content was calculated by comparing the samples with a standard curve generated from the BSA dilution series. Twenty µg of the samples were added to 4x LDS Sample Buffer (Thermo Fisher Scientifc) and 10 x Sample Reducing Agent (Thermo Fisher Scientific) and frozen at -20°C. The remaining native samples were stored at -80°C.

2.2.5.3 SDS-PAGE and protein transfer

The proteins were separated using a SDS-PAGE electrophoresis technique. The gel (NuPAGE 4-12% Bis-Tris GEL, # NP0329BOX, Thermo Fisher Scientific) was installed in the electrophoresis chamber and filled with electrophoresis buffer. If there were gel residues in the pockets after removing the comb, they were washed out with buffer. 20 µg of each protein sample was pipetted into the wells immediately after samples, already mixed with LDS Sample Buffer and Sample Reducing Agent, were boiled for 10 minutes at 70 °C in a block thermostat (Techne). One of the pockets was filled with 3.5 µg band marker to detect the size of the protein bands (Prestained Protein Lader, # 01147545, Thermo Fisher Scientific). The samples were separated at room temperature with voltages of 70 V for the loading gel and 100 V for the running gel (PowerPacTM HC High-Current Power Supply, Bio Rad Laboratories).

The separated proteins were transferred to a polyvinylidene difluoride (PVDF) membrane (Bio Rad Laboratories) for further analysis of antibodies using a tank blotting strategy [82]. To reduce hydrophobic interactions with the transfer buffer, the PVDF membrane was first activated in 100% methanol for 1 minute. After the electrophoresis was complete, the gel was removed, the loading gel discarded, and the running gel placed in the transfer buffer for a short time to remove any electrophoresis buffer that might have remained and interfere the transfer. The gel and the PVDF membrane were then placed between two Whatman® filter papers (GE Healthcare), which had also been soaked in transfer buffer for a few minutes. The filter papers with the gel were then clamped between two fiber pads in the supplied cassette without any air bubbles. The PVDF membrane was installed on the anode side. The transfer chamber was filled with the chilled transfer buffer (Thermo Fisher Scientific). A magnetic stirring bar (GLW) was inserted at the bottom of the transfer chamber and set to the highest speed by a magnetic stirrer (GLW) to maintain an even temperature and ion distribution on the transfer sandwiches. Proteins were transferred over a period of two days at 4°C with an applied current of 40 mA per gel.

The PVDF membrane was immersed in 5% milk in PBS (blocking buffer) for 1 hour (AppliChem) to prevent non-specific binding of the antibodies to the membrane. The primary antibody diluted in blocking buffer as listed in Table 3 was then incubated at 4°C overnight. The membrane was washed three times for 10 minutes with 0.1% Tween (Sigma Aldrich) in PBS to thoroughly eliminate non-specifically bound primary antibodies. The membrane was then incubated with secondary antibody diluted in 5% skim milk as described in Table 3 for 20 minutes.

After the incubation with the secondary antibody, the membrane was washed three more times for a total of 10 minutes with 0.1% Tween/PBS before the 2 minute-incubation in 10 ml of a chemilumiscence solution freshly mixed from two components (ECL I 5ml and ECL II 5ml). The FluorChem FC2 Multi-Imager II (Alpha Innotec) was used for detection, and ImageJ for analysis of protein bands.

2.2.6 Wound healing assay

A special cell culture vessel with two separate chambers (2 well silicone insert, Ibidi GmbH) was used to demonstrate the ability of the cell lines to migrate as published previously [83]. The two chambers are formed by silicone inserts that can be removed without leaving any residue, creating a defined 500 µm wide cell-free gap. After seeding, the cells were cultivated in their individual chambers for a few days until a confluent cell monolayer was formed. A Keyence BZ9000 microscope was used to capture the first image of the gap after the silicone insert was removed and 1% FCS DMEM was added. The migrating cells were photographed after 24 and 48 hours. The percentage of cell free area relative to the initial cell free area was then calculated using BZ-II-Analyzer software (Keyence).

2.2.7 ECM Adhesion assay

The ECM Cell Adhesion Array Kit (Merck) was used to investigate cell adhesion to various ECM components. This is a 96 well plate assay that has been divided into twelve 8-well strips. The reaction strips (8 wells per cell line) were rehydrated in PBS according to the manufacturer's instructions. Each strip has seven wells coated with different human ECM proteins and one control coated with BSA. Relative adhesion was determined by seeding 1.0 x 10^6 cells in serum-free DMEM. The medium was removed after one hour of incubation at 37°C in a 5% CO_2 and 21% O_2 incubator, and non-adherent cells were removed by washing twice with the assay buffer. To stain the cells, 100 µl Cell Stain Solution was added per well. The stain solution was removed after 5 minutes, and the cells were washed with distilled water. 100 µl of Extraction Buffer were added after the dishes had been briefly dried at RT. The absorbance was measured with a microplate reader (Tecan) at a wavelength of 540–570 nm.

2.2.8 Tube formation assay

Tube formation assay can be used to assess the angiogenic potential of endothelial cells *in vitro*. The Matrigel® matrix (Corning) has similar components to the mammalian ECM. Matrigel stored at -20°C was thawed overnight at 4°C. Handling of the Matrigel® was performed on ice [84]. To induce angiogenesis, 20 ng/ml of VEGF (Vascular Endothelial Growth Factor, Thermo Fisher Scientific) was added to Matrigel®. Each

well in a 24-well plate was filled with 300 µl of Matrigel® without bubbles, and the gel polycondensation reaction was carried out at 37°C for one hour. 500 µl of a cell suspension containing 2 x 10^5 cells per ml was added to each well. Images were acquired using a Keyence BZ9000 microscope after 6–18 hours of incubation at 37°C. The parameters of the formed capillaries were analysed with the MetaVi Lab (Ibidi GmbH) software.

2.2.9 Measurement of Transendothelial Electrical Resistance (TEER)

Cell lines were grown to confluence on 24-well Trans-well™ inserts coated with Speed coating solution (ThinCert, pore size 0.4µm, Greiner Bio-One) for 7 days. The culture medium was changed every two to three days. On the seventh day, cell culture medium with 1% FCS was applied. 24 hours later the TEER measurements with a chopsticks electrode were performed (World Precision Instruments Inc.). The resistance of the empty Trans-well™ was subtracted from the measured value before the final calculation of the TEER in Ω cm^2.

2.2.10 Measurement of cell permeability

The cells were grown to confluence on 24-well Trans-wells™ and differentiated with 1% FCS DMEM for 24 hours. 10 µM fluorescein sodium salt (Sigma-Aldrich) with a molecular size of 376 Da was mixed with the Ringer-Hepes buffer. To measure the paracellular flux, 500 µl of fluorescein solution was added to the Trans-well™ insert and incubated at 37°C for one hour. The lower chamber was filled with Ringer-Hepes buffer (1.5ml/well). Samples were taken from the lower chamber every 20 minutes and from the upper chamber after 1 hour and the fluorescence was measured in the microplate reader (Tecan) with an excitation of 485 nm and an emission of 535 nm. The permeability of the cells was determined by comparison to empty Trans-wells™ and in correlation with the initial fluorescein concentration.

2.2.11 Immunohistochemistry

The wild type (WT) and Tjap1 knock-down (KD) cEND cells were seeded on coverslips and were grown to confluence for 6 days. DMEM containing 1% ssFCS was added for 24 hours to increase barrier properties of the cells. After a PBS wash, the cells

were fixed in ice-cold methanol for 10 minutes. The coverslips were then blocked with 5% porcine serum (Normal Swine Serum, Vector Laboratories) in PBS/BSA for one hour. Next, the primary antibodies diluted in 5% porcine serum in PBS/BSA were added and incubated at 4°C overnight in the dark. To visualize the nuclei, DAPI (Roche) 1:100 was added to the primary antibody. The coverslips were washed with PBS/BSA three times the next day, then the secondary antibody (in case of using non-conjugated primary antibody) was added diluted 1: 500 with 5% porcine serum in PBS/BSA for 1 hour. The coverslips were washed with PBS/BSA three times. The coverslips were applied to slides with a drop of mounting solution followed by a one-hour light-protected incubation at room temperature (Vectashield, Vector Laboratories). Images were acquired using a Keyence BZ9000 fluorescent microscope (Keyence).

2.2.12 Statistics

In our experiments we normalized the data to non-transfected cells (the wild type cEND and cerebEND), which was set as 1. A transfected control vector group (Control) served as an additional control, but was not used for validation purposes. All experiments were performed at least three times. The measurement for two groups was analyzed with a student's t-test if distributed normally. Multiple measurements of more than two groups were analyzed by one-way analysis of variance (ANOVA) followed by the Bonferroni post-hoc test if distributed normally. Each data set was compared to the control (wild type cEND or cerebEND) and statistically significant results were marked with asterisks. Further significances between groups are additionally indicated in the graphics. Differences were considered significant when $P<0.05$. Statistical analysis of data was performed with Sigma Plot 12.5. All data are presented as mean ± s.e.m.

3. Results

3.1 Generation of Tjap1 KD cEND and cerebEND models

To examine the role of Tjap1 at the BBB, its expression was knocked-down using Pilt shRNA Plasmid in mouse cEND and cerebEND cell lines. The knock-down of Tjap1 (Tjap 1 KD) was evaluated at the protein and mRNA levels after stably transfecting the cells with Pilt shRNA-expressing plasmid. The significant Tjap1 knock-down was observed at protein and mRNA level in cEND and cerebEND (Figure 3A). After immunostaining the cerebEND cells with the antibodies, a reduced signal for Jam-3 was seen in the Tjap1 KD cells (Figure 3 B). ZO-1 showed slightly stronger staining in the Tjap1 KD cells (Figure 3 B). In addition, we analyzed the expression of proteins and mRNA of ZO-1 (Tjp-1), Jam-3, and claudin-5 in cEND cell line. The expression of ZO-1, Jam-3 and claudin-5 was higher at both protein and mRNA level as shown in Figure 3 C-D, while occludin expression was significantly lower at the mRNA level but not at the protein level (Figure 3 C-D).

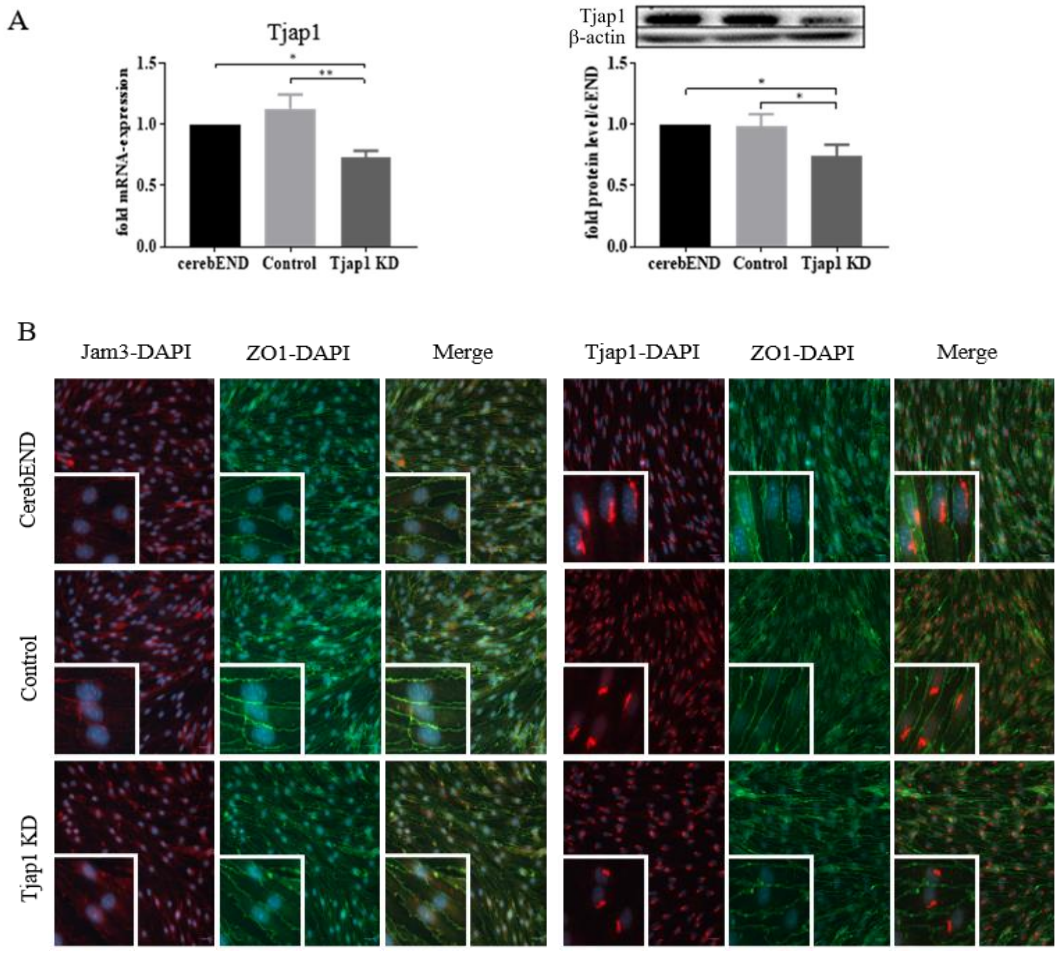

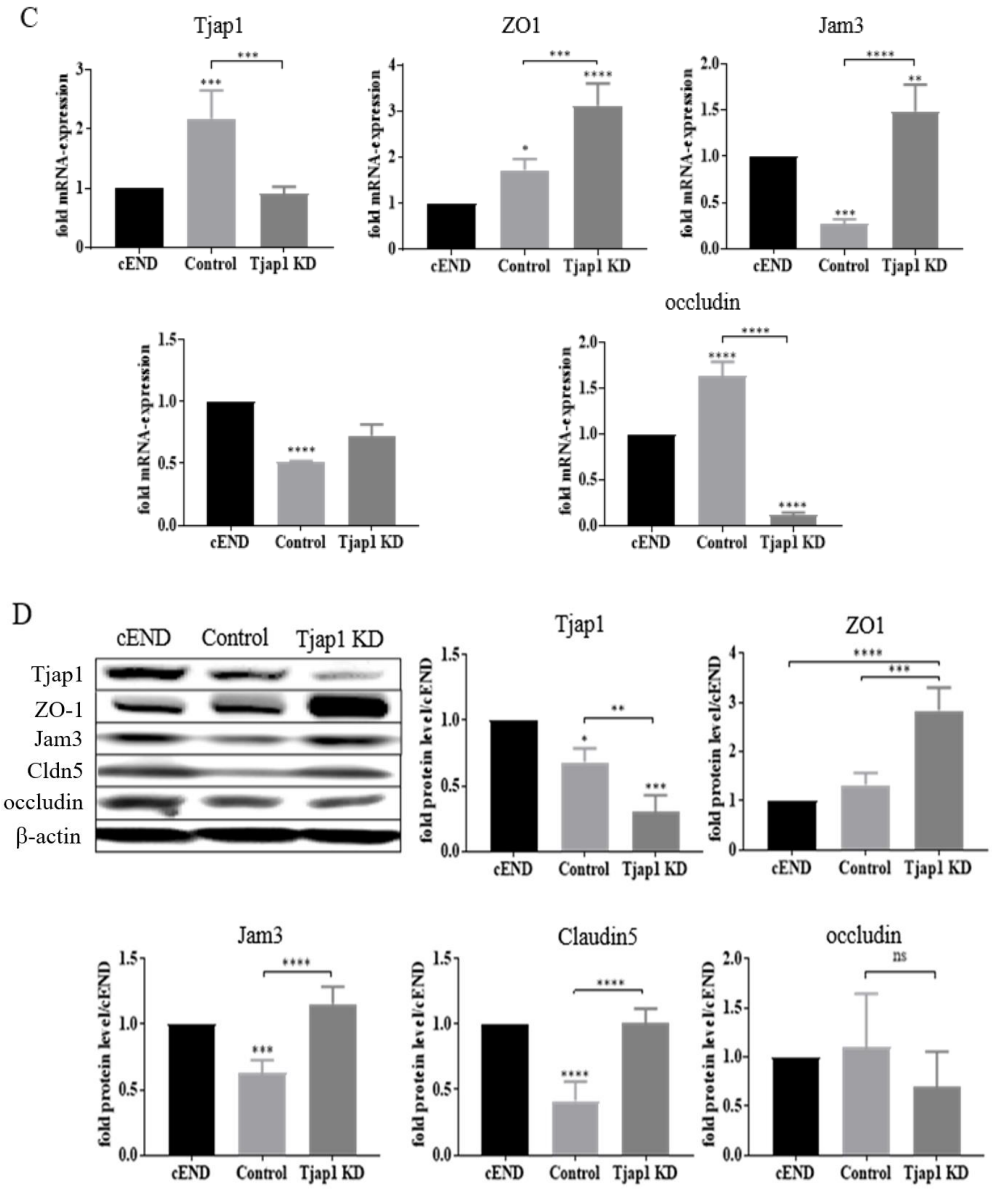

Figure 3: Expression changes in Tjap1 Knock-down (KD) cells compared to control cells. (A) The expression of Tjap1 in the wild type and transfected cerebEND cells (cerebEND, control and Tjap1 KD) at the protein and mRNA level. (B) Immunohistochemical staining of the cerebEND cells. The images were taken with the Keyence BZ9000 fluorescence microscope, scale bars, 20µm. The expression of Tjap1 and the associated proteins BBB proteins (ZO-1, Jam-3, claudin-5 and occludin) in cEND and transfected cell lines (cEND, Control and Tjap1 KD), assessed by qPCR (C) and immunoblotting（D). ß-actin (Western blot) and calnexin (qPCR) were used as endogenous controls. The expression levels of the transfected cells are shown as the fold-change of the wild type cells, which was set to 1. Statistical analysis using ordinary one-way ANOVA. (ns: not significant, *=P<0.05, **=P<0.01, ***=P<0.001, ****=P<0.0001, n=3).

3.2 Altered function of cerebEND/cEND cells with Tjap1 KD

3.2.1 Effect of Tjap1 KD on paracellular permeability

To investigate the effects of Tjap1 KD on the barrier properties of endothelial cells, the TEER and the fluorescein permeability were investigated. The TEER of the Tjap1 KD cells was lower than that of the wild type and control vector cells. The permeability of the Tjap1 KD cells was higher than that of the other groups. TEER was measured in Ωcm^2 and was normalized to wild type cells (Figure 4A). To measure permeability, paracellular flow of fluorescein was measured as described. The wild type cerebEND and cEND and transfected (control and Tjap1 KD) cell lines were cultured in Trans-wells™ for seven days before the experiments were performed. The permeability of the control and Tjap1 KD cells was calculated as a fold of the permeability of wild type cells, which was set as 1. The permeability of the Tjap1 KD cells was increased (Figure 4B).

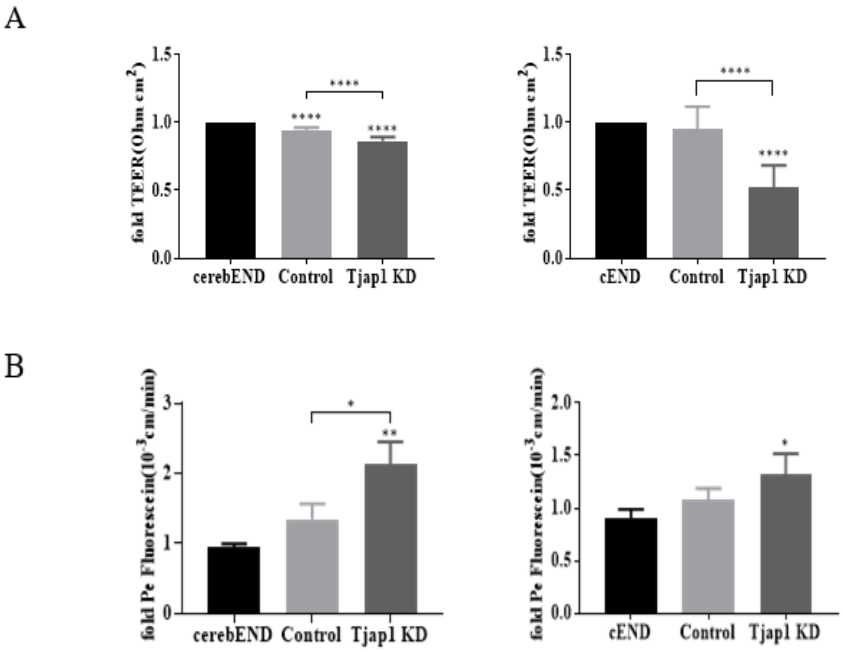

Figure 4: Barrier properties of Tjap1 Knock-down in cerebEND and cEND cell lines. (A) Transendothelial electrical resistance. Shown are TEER values normalized to wild type cells set to 1. (B) Paracellular permeability of cerebEND and cEND cell lines. The permeability values of transfected cells were normalized to wild type cells which were set to 1. Statistical analysis using ordinary one-way ANOVA. (*=P<0.05, ****=P<0.0001, n=3).

3.2.2 Effect of Tjap1 KD on cell viability

In 96 well plates, the same amount of cells were seeded for MTT assay as described in Materials and Methods. The measured absorbance correlates with the amount of the living cells in the well. Tjap1 KD cerebEND and cEND cells showed lower viability than the wild type and control cEND and cerebEND (Figure 5).

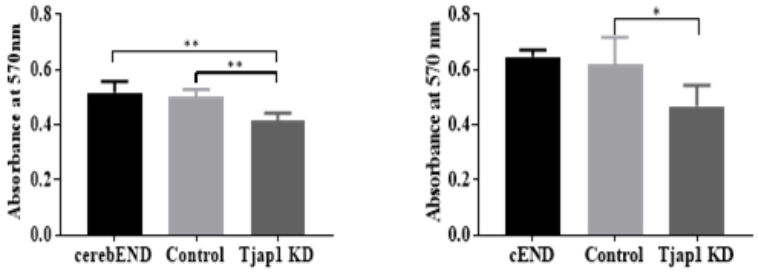

Figure 5: Lower cell viability of Tjap1 Knock-down (Tjap1 KD) in cerebEND and cEND cell lines. The cell viability was measured by MTT. Statistical analysis using ordinary one-way ANOVA. (*=P<0.05, **=P<0.01, n=3).

3.2.3 Effect of Tjap1 KD on cell proliferation and migration capacity

The BrdU Cell Proliferation Assay was used to measure the proliferation rate of wild type and transfected cerebEND and cEND. After cell passaging, 5,000 cells were seeded in 96 well plate. After the cells attached, the BrdU label was added. After 24 hours the BrdU labeling was detected with respective antibody and the absorbance was measured at 450/540. The Tjap1 KD cells proliferated significantly slower than wild type cerebEND and cEND cells (Figure 6A). Next, a wound healing approach was used to assess the migration rate of the cell lines. The cells were first grown in chambers separated by a silicone insert. After removal of the separation chambers, a defined gap of 500 µm was created (Figure 6B-C). The cell free area was measured at time 0 and 48 hours. Tjap1 KD migrated faster than control and wild type cells.

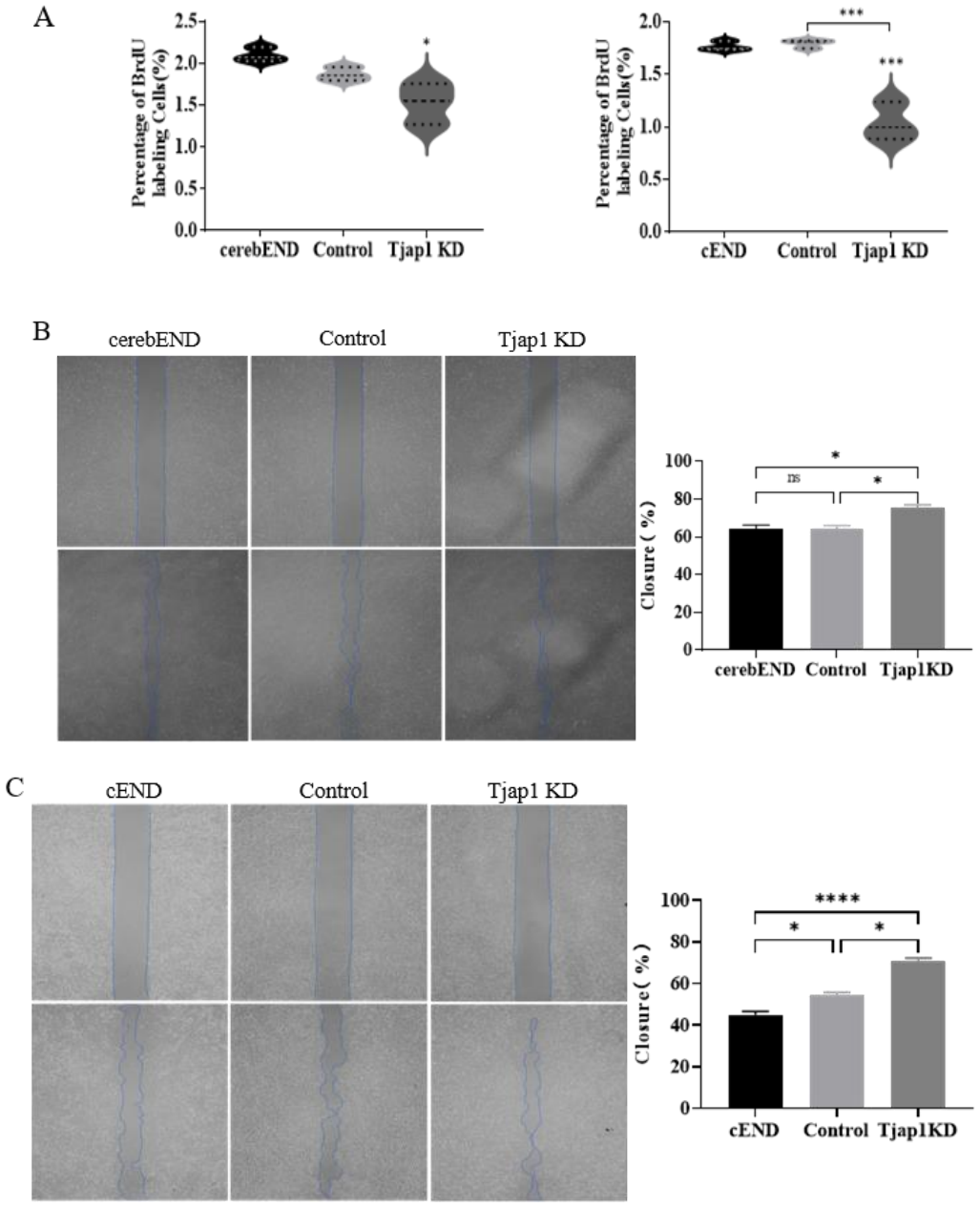

Figure 6: Cell proliferation and migration ability of Tjap1 Knock-down (Tjap1 KD) in cerebEND and cEND cell lines. (A) Proliferation assay. BrdU incorporation was measured in different cell lines. Tjap1 KD cerebEND and Tjap1 KD cEND cells showed lower proliferation rate than wild type (cerebEND and cEND) and control cells (cEND). (B) Wound healing assay of wild type and Tjap1 KD cerebEND cells. The cells were photographed immediately after removal of the silicon insert (0h) and after 48h. The cell free area was measured and the migration rate was calculated. (C) Wound healing assay of wild type and Tjap1 KD cEND cells. Mean values and standard deviation are shown. Statistical analysis using ordinary one-way ANOVA. (ns: not significant, *=P<0.05, ***=P<0.001, ****=P<0.0001, n=3).

3.2.4 Effect of Tjap1 KD on tube formation

The ability of endothelial cell lines to form tubes *in vitro* was examined by seeding the cells on Matrigel®. Endothelial cells form vessel-like structures (so-called tubes) in this gel, which branch and form rounded structures (so-called loops) (Figure 7). Four passages of wild type, control vector and Tjap1 KD cEND cells were analyzed. The assay was not performed in cerebEND. The following parameters were determined using MetaVi Lab software (Ibidi GmbH): number of loops, average area, length of tubes and number of branches. Tjap KD cells showed a significantly reduced ability to form tubes compared to control and wild type cEND (Figure 7).

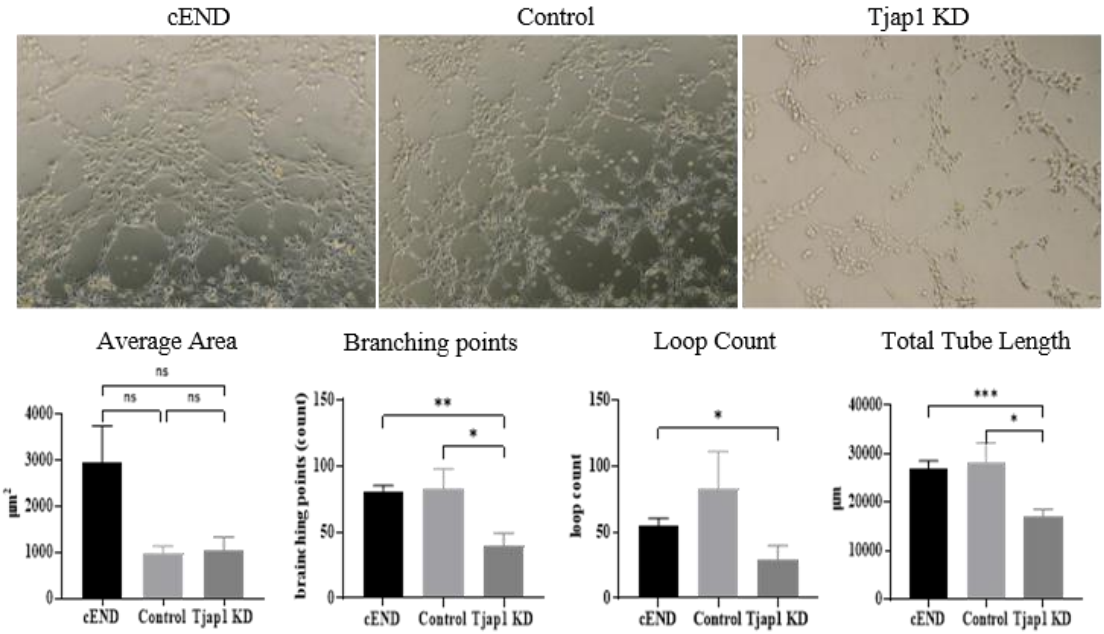

Figure 7：Tube formation assay of Tjap1 Knock-down in cEND cell lines. (A) Growth of cEND, control and Tjap1 KD cells in Matrigel. The images were taken after 6 h incubation at 37°C with the Keyence microscope at 10 x magnification. Representative low magnification images (10×) of tubes formed by cells are shown. Total tube number, branching points and tube length were assessed by MetaVi Lab software. Values are means ± SEM, statistical analysis using ordinary one-way ANOVA (ns: not significant, *=P<0.05, **=P<0.01, ***=P<0.001, n=3).

3.2.5 Effect of Tjap1 KD on cell adhesion

The ECM Cell Adhesion Assay Kit was used to determine adhesion to various components of the ECM. Three consecutive passages of wild type cerebEND and

control and Tjap1 KD cells were analyzed in comparison. No statistically significant differences in adhesion were observed between the cell lines (Figure 8).

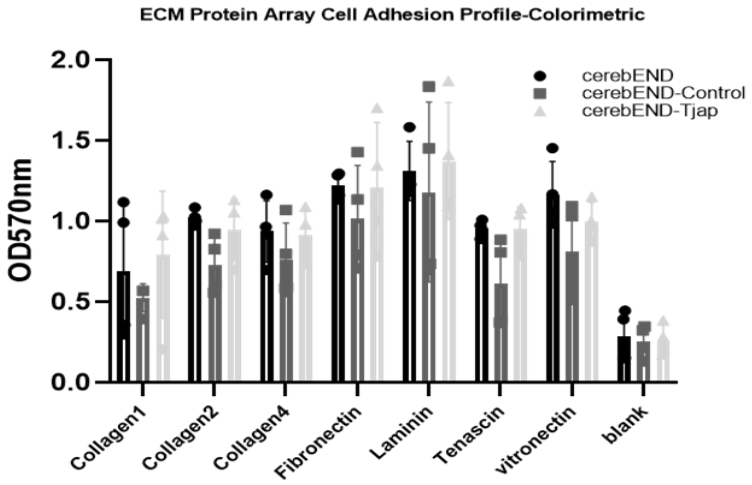

Figure 8: Cell adhesion ability of Tjap1 Knock-down in cerebEND cell lines. Values are means ± SEM, Statistical analysis using ordinary one-way ANOVA, no statistical differences were detected (n=3).

3.3 Effects of Tjap1 KD on metabolic activity and barrier properties under OGD conditions

3.3.1 Effect of Tjap1 KD on barrier properties under OGD conditions

TEER and paracellular permeability to fluorescein were analyzed to assess the effect of OGD and Tjap1 KD on endothelial cells barrier properties. OGD-treated cells showed lower TEER values than the cells grown under normal conditions (Figure 9A). In addition, the permeability of OGD-treated cells was higher than that of the cells cultured under normal conditions (Figure 9B). TEER and permeability values are shown as a fold of cells grown under normal culture conditions. Interestingly, the Tjap1 KD showed significantly lower TEER and higher permeability values as compared to wild type and / or control cells.

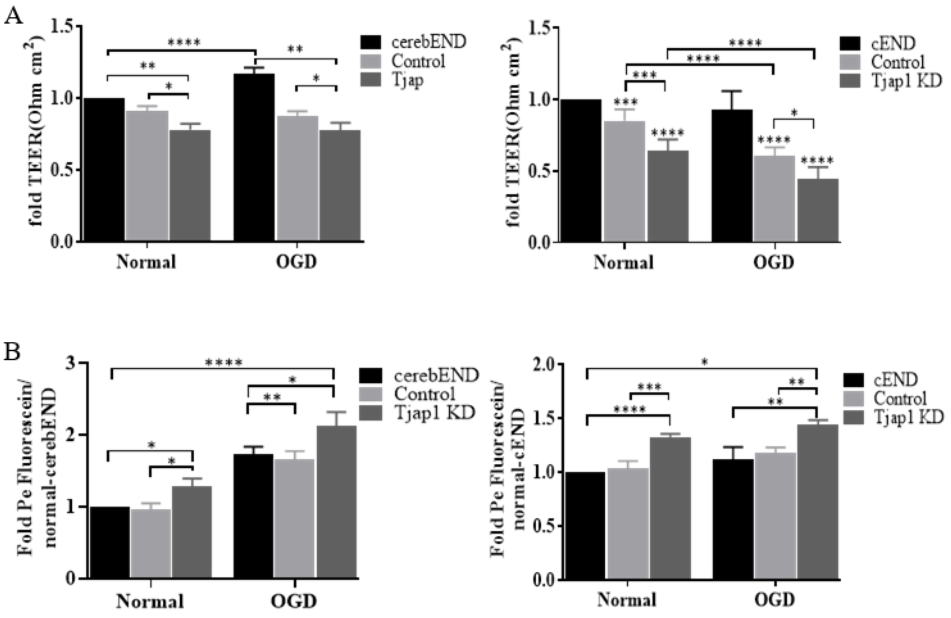

Figure 9: Barrier properties under OGD conditions in cerebEND and cEND cell lines. (A) Transendothelial electrical resistance. (B) Transcellular permeability measurement. Values of transfected cells were normalized to wild type cells set to 1. Values are means ± SEM, Ordinary one-way ANOVA was used in each group, Two-way ANOVA was used between two conditions (*=P<0.05, **=P<0.01, ***=P<0.001, ****=P<0.0001, n=3) for statistical analyses.

3.3.2 Effect of Tjap1 KD on cell viability under OGD conditions

We intended to confirm the impact of OGD on cell viability, as previously demonstrated. The viability of both cerebEND and cEND cells was decreased under OGD conditions as compared to the normal conditions (Figure 10). Tjap1 KD cEND and cerebEND showed significantly lower viability and metabolic activity compared to the respective wild type and control cells.

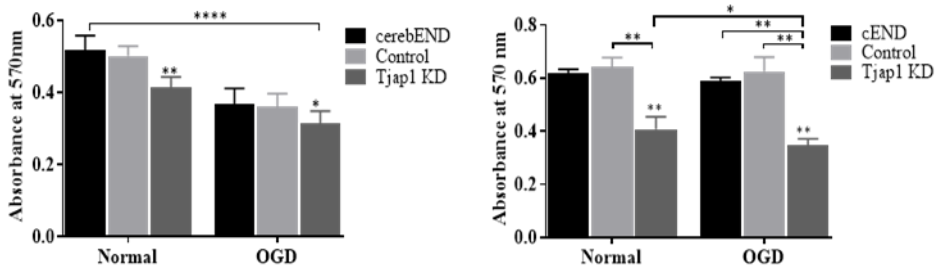

Figure 10: Cell viability under OGD conditions in cerebEND and cEND cell lines. MTT assay for estimation of cell viability under normal and OGD-conditions was performed with wild type, control and Tjap1 KD cerebEND and cEND cells. Values are means ± SEM, Ordinary one-way ANOVA was used in

each group, Two-way ANOVA was used between two conditions (*=P<0.05, **=P<0.01, ****=P<0.0001, n=3) for statistical analyses.

3.4 The effect of OGD conditions on tight and adherens junctions proteins

Tight junctions (TJs) and adherens junctions (AJs) [13], affect the barrier function of endothelial cell lines. The changes at the mRNA and protein level of TJs and AJs proteins correspond to changes in barrier tightness.

3.4.1 The effect of OGD conditions on tight junctions proteins

TJs are mainly composed of transmembrane proteins (including claudin-1,-5,-12, occludin, and junctional adhesion molecule-A) that close the gap between cells, cytoplasmic scaffolding proteins (including zonula occludens proteins ZO-1-3) that physically support the TJs and are connected to the actin cytoskeleton [85]. We evaluated the expression of TJs proteins in cerebEND and cEND cells by qPCR and WB to analyze the effects of Tjap1 KD in OGD (Figure 11).

The expression of Tjap1 was decreased in the Tjap1 KD group in cerebEND and cEND cells at both mRNA and protein levels, but there was no significant difference in Tjap1 expression among normal and OGD conditions. At the protein level, the expression of Tjap1 was significantly decreased in the OGD-treated group compared to normal culture conditions (Figure 11A). The expression of occludin in Tjap1 KD cerebEND and cEND was significantly downregulated at the mRNA level, but there was no difference between the OGD and the normal culture conditions groups. In addition, there were no significant changes at the protein level of occludin (Figure 11B).

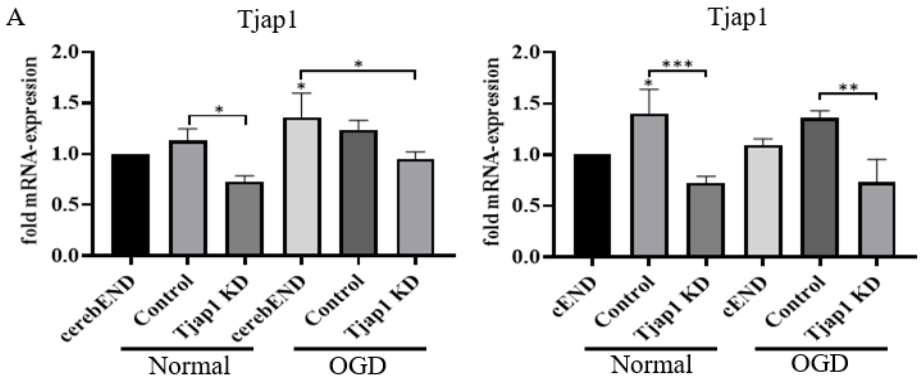

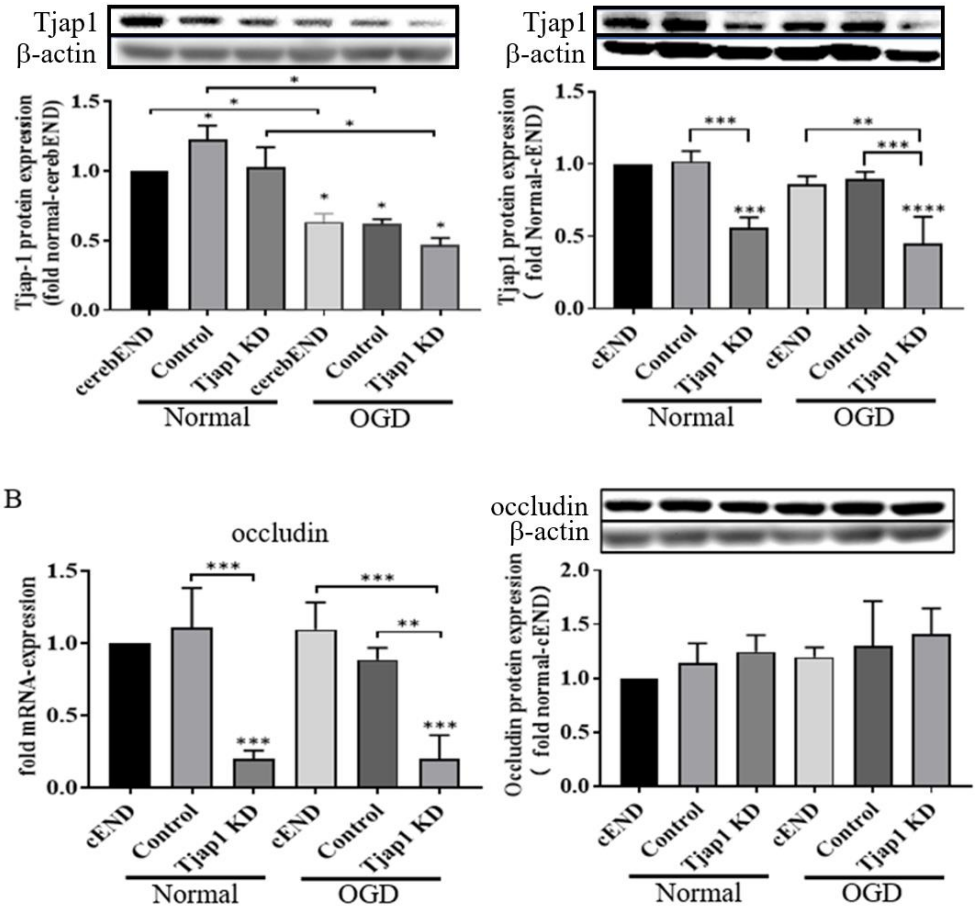

Figure 11: The Effect of OGD condition on tight junction protein expression. The mRNA and protein expression was detected by qPCR and WB. (A) The expression of Tjap1 in cerebEND and cEND cell lines. (B) The expression of occludin in cEND cell line. ß-actin (Western blot) and calnexin (qPCR) were used as endogenous controls. The expression levels of the transfected cells are shown as the fold change of the wild type cells, which was set to 1. Values are means ± SEM, statistical analysis using ordinary one-way ANOVA (*=P<0.05, **=P<0.01, ***=P<0.001, ****=P<0.0001, n=3).

Claudin-1 expression was reduced at the mRNA and protein level in Tjap1 KD cerebEND and cEND, showing no significant difference between normal and OGD conditions (Figure 12A). Claudin-5 expression was reduced in the cerebEND Tjap1 KD cell line, but there was no significant difference between normal and OGD conditions. Claudin-5 expression was significantly increased in the cEND Tjap1 KD cell line with no difference between normal and OGD conditions (Figure 12B). Claudin-12 expression was also different between cerebEND and cEND, with significantly increased expression in Tjap1 KD cerebEND and significantly decreased expression in

Tjap1 KD cEND, with no differences observed between normal and OGD conditions (Figure 12C).

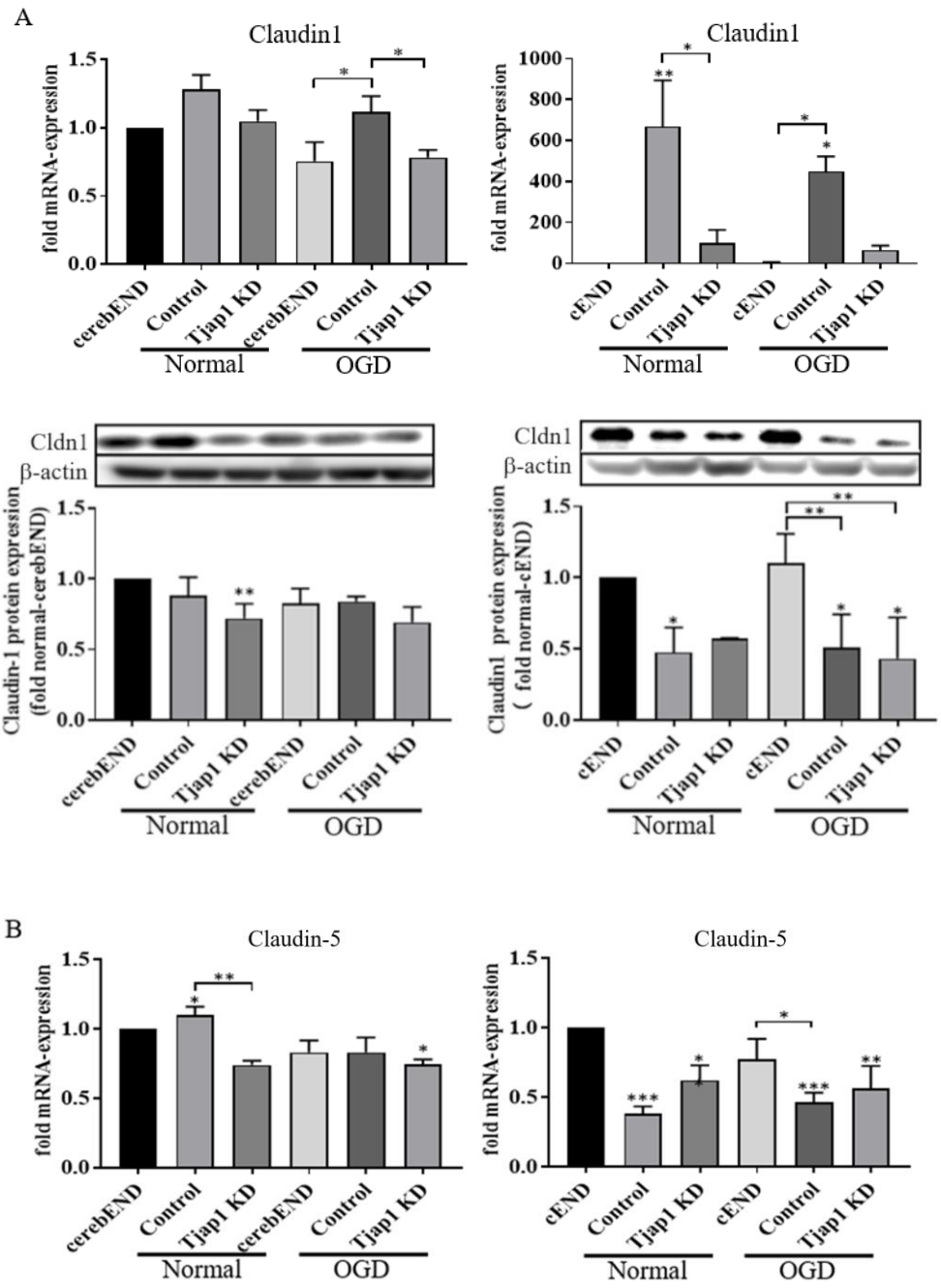

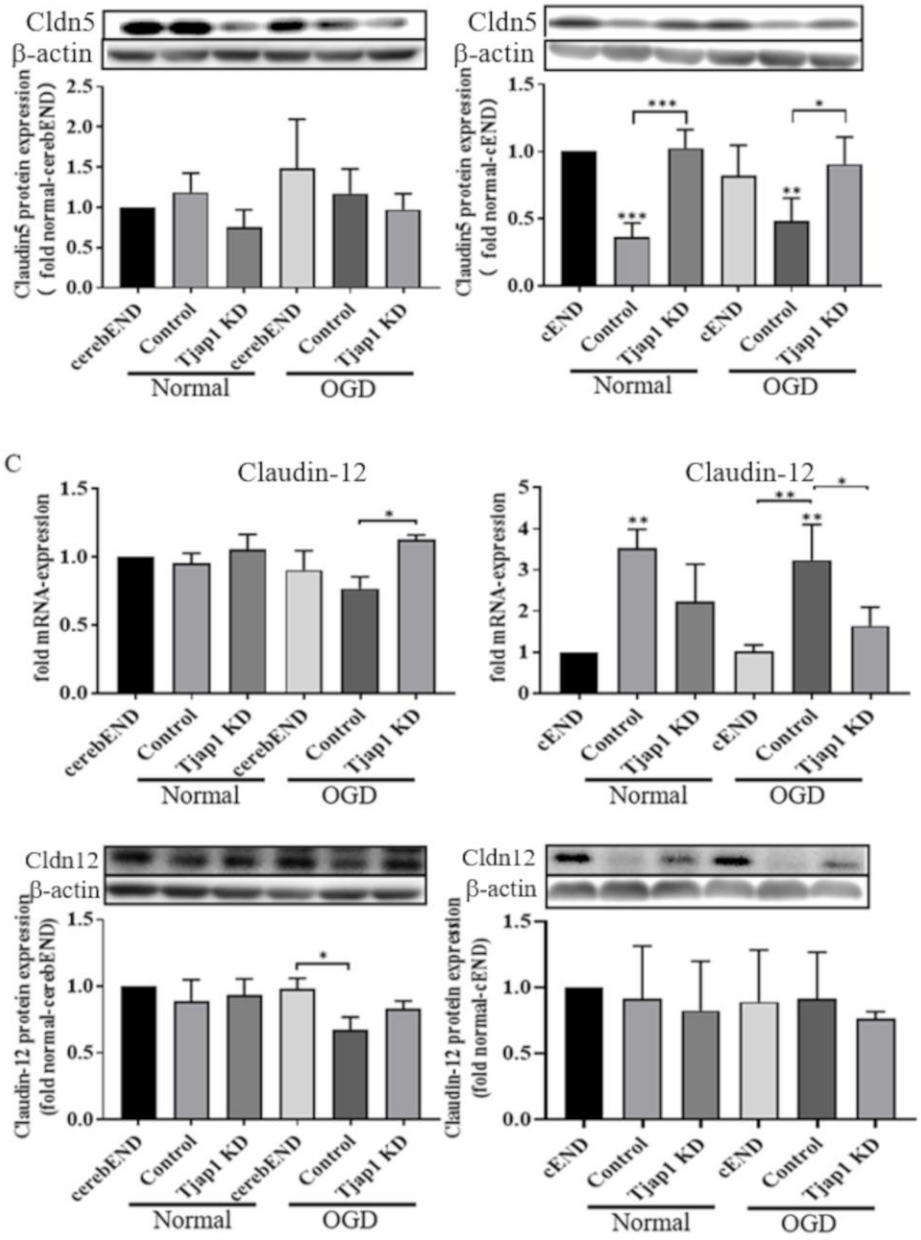

Figure 12: The Effect of OGD on tight junction proteins. The mRNA and protein expression was detected by qPCR and WB. (A) The expression of claudin-1. (B) The expression of claudin-5. (C) The expression of claudin-12. ß-actin (Western blot) and calnexin (qPCR) were used as endogenous controls. The expression levels of the transfected cells are shown as the fold change of the wild cells, which was set to 1. Values are means ± SEM, Statistical analysis using ordinary one-way ANOVA (*=P<0.05, **=P<0.01, ***=P<0.001, ****=P<0.0001, n=3).

ZO-1 expression was significantly increased at both mRNA and protein level in Tjap1 KD cerebEND and cEND cells. However, there was no difference between the normal and OGD conditions (Figure 13A). Jam3 expression in Tjap1 KD cerebEND cells was reduced at both mRNA and protein level, showing no difference between normal and

OGD conditions (Figure 13B). In cEND cells, Tjap1 KD resulted in increased Jam3 expression.

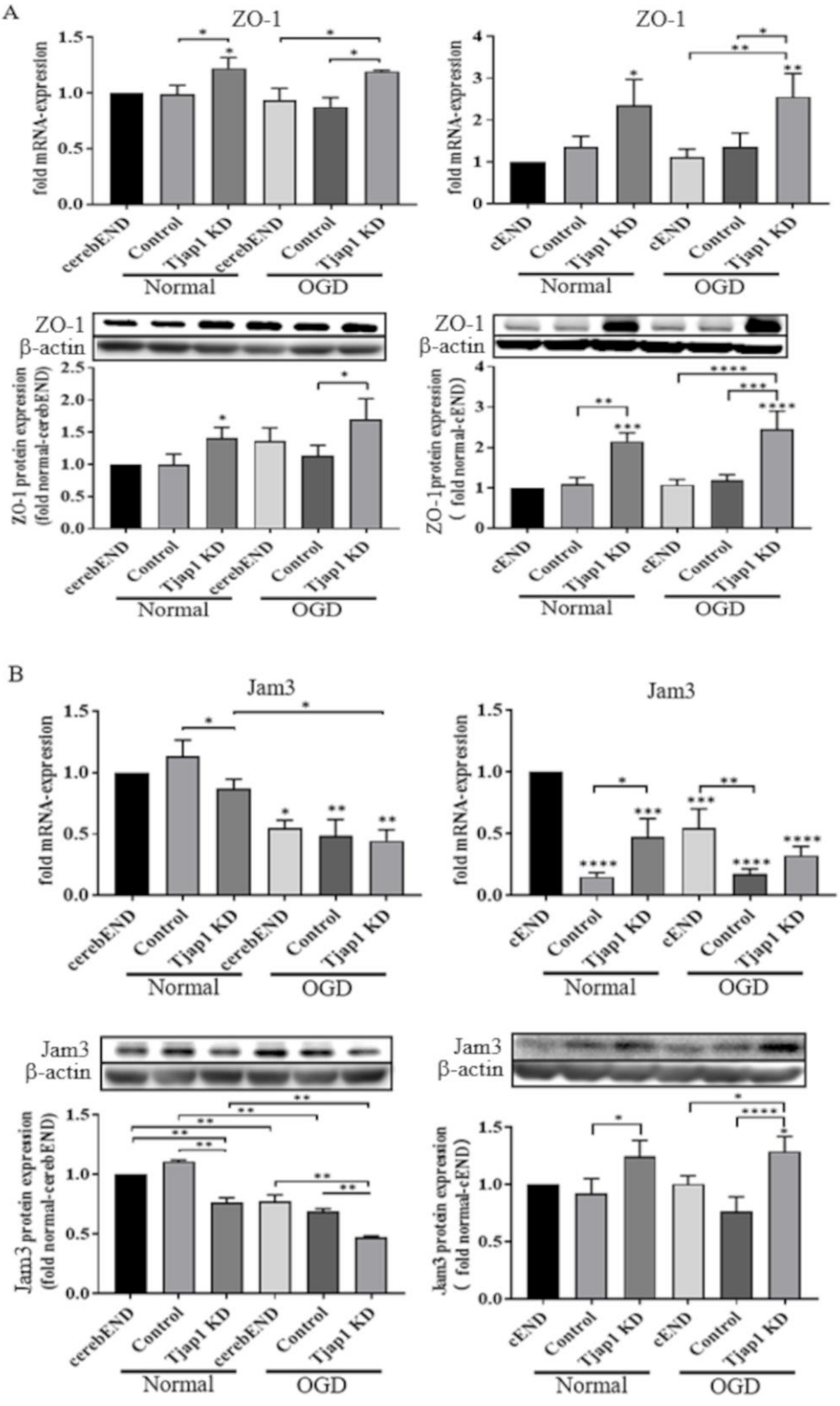

Figure 13: Effect of OGD on tight junction proteins. The mRNA and protein expression was detected by RT-PCR and WB. (A) The expression of ZO-1. (B) The expression of Jam3 ß-actin (Western blot) and calnexin (qPCR) were used as endogenous controls. The expression of the transfected cells is shown as the fold change of the wild type cells, which was set to 1. Values are means ± SEM, statistical analysis using ordinary one-way ANOVA (*=*P*<0.05, **=*P*<0.01, ***=*P*<0.001, ****=*P*<0.0001, n=3).

3.4.2 The effect of OGD conditions on adherens junction proteins

In addition to the TJs, the junctional complex includes the AJs. Vcam1 expression was reduced at the mRNA level in both cerebEND and in cEND Tjap1 KD cells lines but increased at the protein level. However, expression at protein levels of both cell lines were increased, but there was no statistically significant difference (Figure 14A). In cerebEND Tjap1 KD cells, VE-cadherin (Cdh-5) expression was increased at both mRNA and protein levels. However, in cEND Tjap1 KD cells, mRNA expression was reduced while protein expression was increased. No differences between normal and OGD conditions could be observed (Figure 14B).

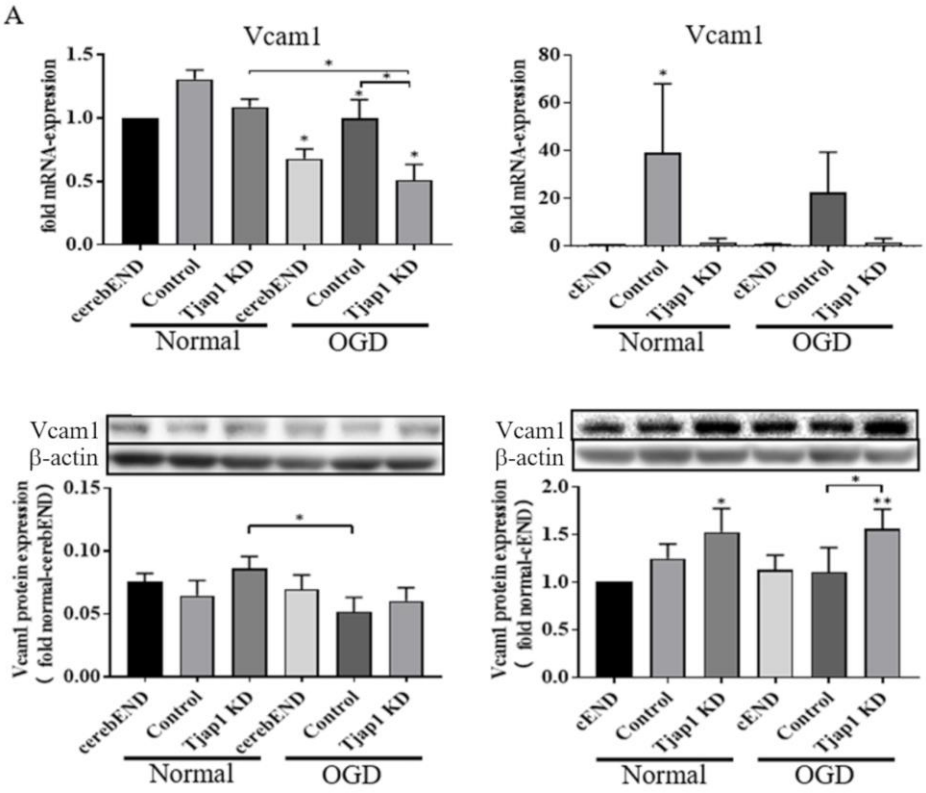

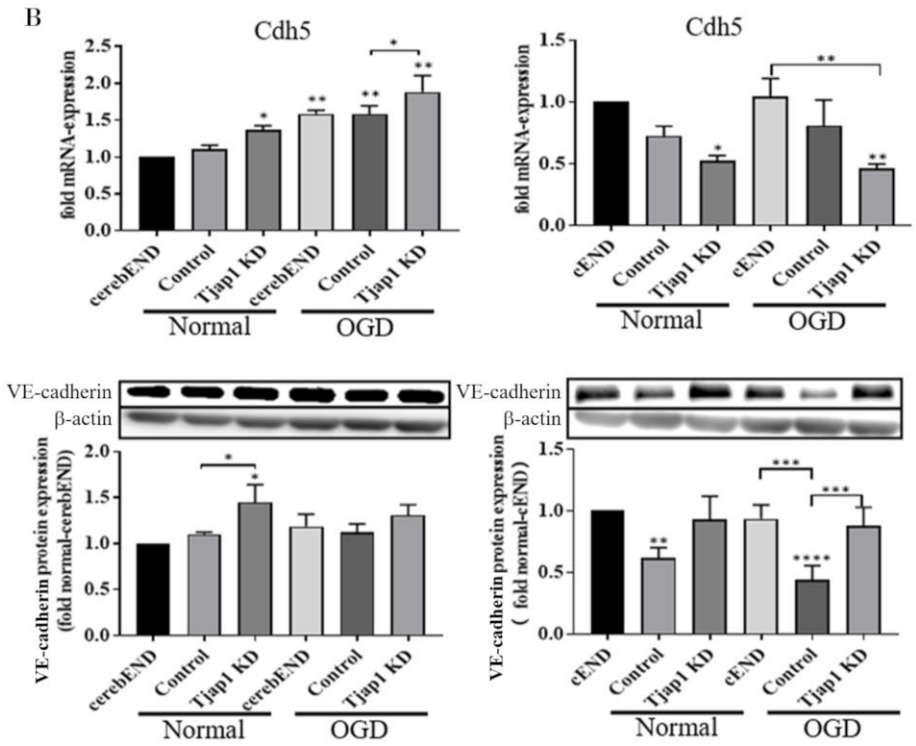

Figure 14: Effect of OGD on adherens junction proteins. The mRNA and protein expression was detected by RT-PCR and WB. (A) The expression of Vcam-1. (B) The expression of VE-cadherin. ß-actin (Western blot) and calnexin (qPCR) were used as endogenous controls. The expression of the transfected cells is shown as the fold change of the wild type cells, which was set to 1. Values are means ± SEM, statistical analysis using ordinary one-way ANOVA (*=P<0.05, **=P<0.01, ***=P<0.001, ****=P<0.0001, n=3).

3.4.3 The effect of OGD conditions and Tjap1 KD on inflammatory response

The endothelial cells are activated in response to ischemic stroke and trauma, releasing pro-inflammatory mediators and upregulating cell adhesion molecules. Ccl-2, Ccl-5, and Csf-3 expression was reduced in cerebEND Tjap1 KD cells compared to the control cells, but there was no difference between normal and OGD conditions. Similar expression changes were observed in cEND Tjap1 KD cells (Figure 15 ABCD).

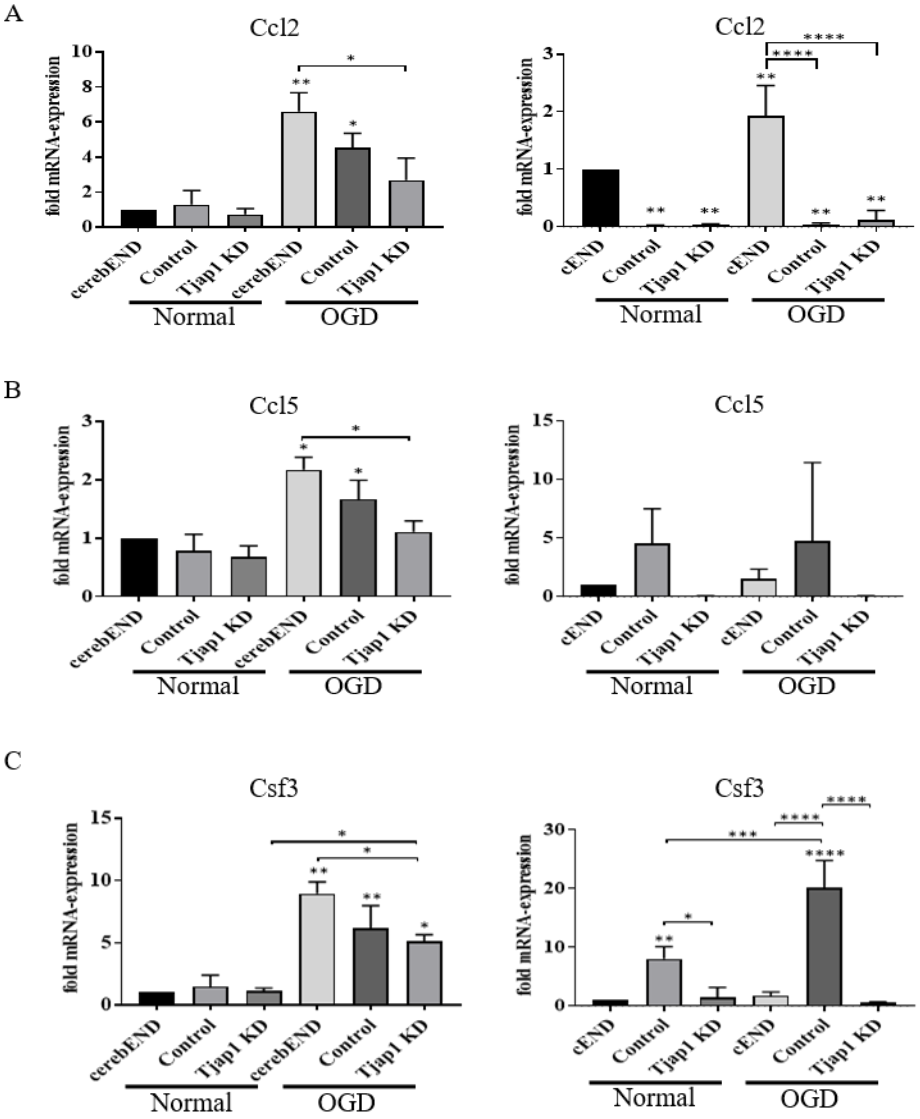

Figure 15: Effect of OGD and Tjap1 KD on inflammatory response. The mRNA expression was detected by qPCR. (A) The expression of Ccl-2. (B) The expression of Ccl-5. (C) The expression of Csf-3. Calnexin was used as an endogenous control. The expression levels of the transfected cells are shown as the fold change of the wild type cells, which was set to 1. Values are means ± SEM, statistical analysis using ordinary one-way ANOVA (*=P<0.05, **=P<0.01, ***=P<0.001, ****=P<0.0001, n=3).

3.4.4 The effect of OGD conditions and Tjap1 KD on ABC transporter

The ABC transporter protein family consists of 48 members, divided into seven subfamilies based on structural homology. The most notable for BBB function are the P-gp and Mrp. After Tjap1 KD, Mrp1 (Abcc1) expression was significantly decreased at mRNA level compared to the control cells, but there was no difference between normal and OGD conditions (Figure 16A). P-gp (Abcb1a), on the other hand, was

decreased at both mRNA and protein levels in cEND Tjap1 KD cells, with no difference in cerebEND Tjap1 KD cells (Figure 16B).

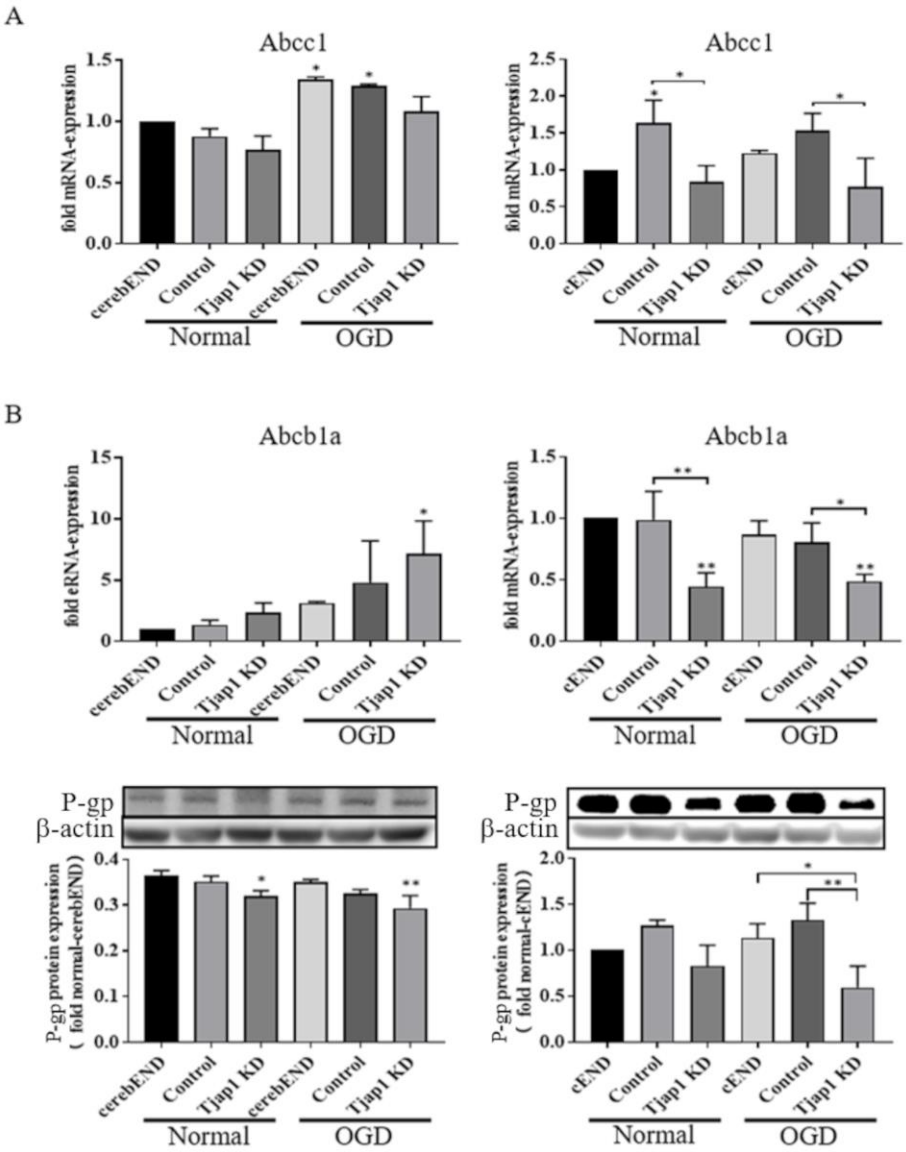

Figure 16: Effect of OGD on ABC transporter expression. (A) The expression of Abcc1 at mRNA level. (B) The expression of Abcb1a at mRNA and protein level. ß-actin (Western blot) and calnexin (qPCR) were used as endogenous controls. The expression levels of the transfected cells are shown as the fold change of the wild type cells, which was set to 1.Values are means ± SEM, statistical analysis using ordinary one-way ANOVA (*=P<0.05, **=P<0.01, ***=P<0.001, ****=P<0.0001, n=3).

3.4.5 The effect of OGD conditions on Timp3

Matrix metalloproteinases are a group of peptidases involved in the degradation of the ECM. Tissue inhibitor of metalloproteinases 3 (Timp3) inhibits matrix metalloproteinases. The changes of BBB permeability are accompanied by breakdown of the ECM. Tjap1 KD led to decreased Timp3 mRNA expression in cerebEND and cEND under OGD conditions (Figure 17A). Similarly, lower Timp3 protein levels were observed in Tjap1 KD cerebEND and cEND cells treated with OGD (Figure 17B).

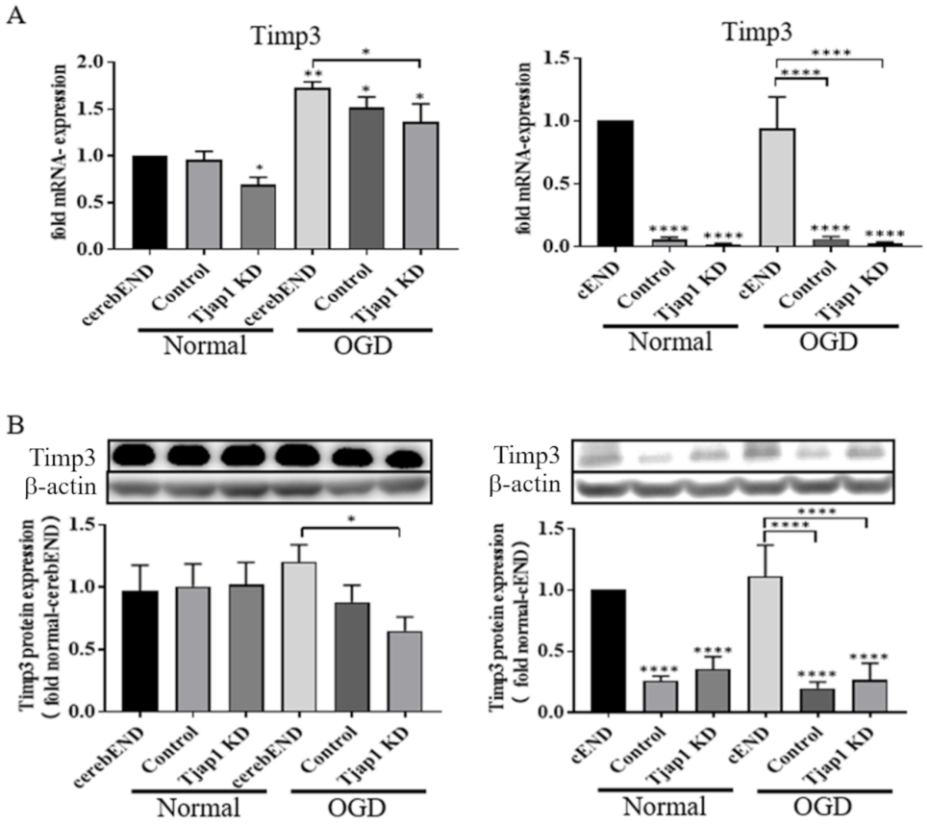

Figure 17: Effect of OGD on Timp3 protein and mRNA expression. The mRNA and protein expression was detected by qPCR and WB. (A) The expression of Timp3 mRNA. (B) The expression of Timp3 proteins ß-actin (Western blot) and calnexin (qPCR) were used as endogenous controls. The expression levels of the transfected cells are shown as the fold change of the wild type cells, which was set to 1. Values are means ± SEM, Statistical analysis using ordinary one-way ANOVA (*=P<0.05, **=P<0.01, ****=P<0.0001, n=3).

4. Discussion

4.1 Tjap1 Knock-down

We used the Tjap1 knock-down method to examine the Tjap1 and its role in BBB properties. Small and short hairpin RNAs, or shRNAs, have the ability to permanently or transiently block the expression of target genes at the RNA level [86]. We generated the cEND Tjap1 KD and cerebEND Tjap1 KD cell lines using stable expression of vectors with shRNAs against Tjap1 mRNA. The gene knock-down was verified by PCR and WB showing that Tjap1 expression was decreased in both cell lines compared to the wild type and control cells. In fact, strong effects on Tjap1 expression were observed at mRNA level. However, at the protein level, only a partial reduction of Tjap1 was observed meaning that Tjap1 function was reduced in the cells but still present at a lower level.

4.2 Barrier properties and regulation of TJ proteins

The BBB, which separates the brain from the blood and regulates the exchange of specific chemicals, is a highly specialized structure. Various neurological diseases are associated with changes in BBB function. Elucidating the mechanism of action of the BBB can be of great benefit in the treatment of diseases, since modifications in the barrier properties of the BBB are major pathways of regression in many pathologies, particularly trauma and stroke. Intercellular TJs, AJs, ABC transporter proteins, release of inflammatory factors from cells and ECM degradation are all associated with regulation of the BBB barrier properties.

Tjap1 is expressed in the Golgi apparatus and is involved in TJ regulation, but its exact role is unclear. This study demonstrated that Tjap1 KD can decrease cell survival in cerebEND and cEND cells (Figure 5) as well as alter their ability to proliferate and migrate. Tjap1 KD appeared to have a negative effect on endothelial cell barrier properties. Tjap1 KD cells show higher fluorescein permeability and lower TEER values compared to wild type and control cells. Yan et al. [87] showed that Tjap1 and claudin-1 expression was elevated when the BBB was dysfunctional. In our case Tjap1 and claudin-1 expression were reduced. In Tjap1 KD cells, the expression of others TJ proteins was also altered. Claudins are transmembrane proteins that bind the membrane

across layers and are essential for the formation and maintenance of TJs [88]. Claudin-5 modulates the paracellular transport of small molecules and is highly expressed in brain capillaries [22]. The polymerization of claudins requires the scaffold protein ZO-1. In addition, ZO-1 and Jam-3 are involved in angiogenesis, barrier formation, and cell migration. The expression of ZO-1 and Jam-3 was similar to that of claudin-5, with increased expression at both the mRNA and protein levels. On the other hand, the function of occludin in TJs is thought to be similar to that of Tjap1, both of which have regulatory roles in late tight junctional action. Occludin expression was significantly downregulated at the mRNA level, although the protein level showed an unstable trend. We believe that either Tjap1 KD alters the function of other highly associated proteins or that this is a compensatory mechanism. Further research is needed to discover the exact mechanism. Meanwhile, an increasing number of studies are now showing that BBB dysfunction is not only caused by an altered expression level of crucial TJ proteins, but rather by the instability of the TJ complex [80], which also explains why some other proteins are expressed differently in Tjap1 KD cells in the opposite direction.

4.3 OGD and Barrier properties

Previous research has demonstrated that hypoxia increases the expression of microRNA 212/132, which in turn compromises the integrity of the BBB [80]. Our results show that hypoxia enhances the reduced cell viability caused by the Tjap1 KD in the cEND Tjap1 KD and cerebEND Tjap1 KD cell lines, although there is no statistically significant difference between the two conditions in the cEND Tjap1 KD cells. At the same time, the barrier properties of the cells changed, with KD cells exhibiting increased fluorescein permeability and reduced TEER values. Compared to normal controls, hypoxia exacerbated BBB dysfunction, although this impact was not statistically significant in the cEND Tjap1 KD cell line. It is possible that this is the case because the two cell lines come from different parts of the brain. The BBB of different brain regions could be regulated in different ways. The local microenvironment, transport systems, enzymes, and extracellular matrix are all altered by the hypoxic environment, further leading to the passage of harmful serum components and immune cells through the BBB, disturbing the CNS homeostasis and negatively affecting the surrounding brain parenchyma.

4.3.1 OGD and TJs

Cell growth, TJ protein expression changes, and cytoskeletal rearrangements are all driven by hypoxia. The results indicate that although Tjap1 KD reduced Tjap1 mRNA and protein expression, consistent with reduced barrier properties, the hypoxic environment was not significantly different from the normal treatment group. This is consistent with the barrier properties after hypoxic treatment and may be related to the duration of hypoxia or reoxygenation time. In addition, it has been shown that members of the TJ protein family respond differently at different time points after hypoxic damage to endothelial cells [89]. However, this was not verified in our experiments.

The role of occludin in epithelial cells has been described as regulatory rather than barrier tightening [90]. The BBB is disrupted by a variety of changes; however, occludin protein expression is a late target. Although occludin mRNA expression significantly decreased in Tjap 1 KD cells, its expression was not significantly different under normal and OGD conditions. In addition, the expression of its proteins was unstable, possibly due to a post-transcriptional regulation that was not examined in this work.

The formation of TJ in brain endothelial cells involves claudin-1, -5, and -12 [22]. Du et al. showed that increased claudin-1 expression improved LPS-induced deterioration in endothelial permeability [91]. The results of our work show that both the mRNA and protein levels of claudin-1 were reduced in Tjap1 KD cells. In addition, hypoxia decreased the expression of claudin-1 mRNA, but with no statistically significant difference compared to normal conditions.

Claudin-5 plays an important role in regulating the permeability of small molecules across the BBB [16]. Claudin-5 seals the barrier, which can engage the homophilic interactions or binding to claudin-3 [92, 93] and claudin-1 [94]. After hypoxic treatment, claudin-5 expression was decreased in the Tjap1 KD cerebEND but did not changed significantly from the normal treatment group. Studies have shown [66, 95] that OGD reduces the expression level of the claudin-5 gene and affects the claudin-5 protein location at the plasma membrane. Nevertheless, claudin-5 expression was increased in

Tjap1 KD cEND at the mRNA and protein levels, again without any apparent differences between the OGD treatment group and the normal treatment group. It is interesting to note that cEND and cerebEND cells did not show the same tendency of claudin-5 expression. This could be related to the fact that the two cell types originate from different areas of the brain.

In addition, we examined claudin-12 expression. Here, the trend was different. Tjap1 KD cerebEND cells showed increased expression, but neither mRNA nor protein level showed a statistically significant difference between groups. Nevertheless, claudin-12 expression in cEND cells was strongly reduced in the Tjap1 KD group but OGD treatment appeared not to differ from the control group. In an animal model of multiple sclerosis, Castro Dias et al. demonstrated that knocking-down claudin-12 resulted in the formation of an intact BBB with no evidence of dysfunction or inflammation. This therefore indicates that claudin-12 is unlikely to be involved in the progression and maintenance of TJ integrity [96].

ZO-1 plays an important role in maintaining the integrity of the BBB. Tjap1 KD cEND cells showed an increased expression of ZO-1 at mRNA and protein levels, however no difference between OGD and normal conditions was observed. Several members of the Jam family interact with scaffold proteins containing the PDZ domain (e.g. ZO-1) to promote maturation of cell-cell junctions and to regulate the production of linking complexes such as TJs and AJs [97, 98]. In the cEND and cerebEND cell lines, Jam-3 expression was different. In Tjap1 KD cerebEND cells, Jam-3 expression was downregulated and OGD treatment further downregulated its expression. In contrast, Tjap1 KD cEND cells showed increased Jam-3 expression with no changes due to OGD. It has been shown that ZO-1 [99] and Jam-3 [100] expression is reduced due to hypoxia. This is consistent with the regulation in cerebEND and correlates with impaired barrier properties of our model. This also demonstrates that the maintenance of the BBB correlates with the stability of the TJs protein complex. Furthermore, Jam-3 and ZO-1 are direct targets of microRNA-212/132 and are also post-transcriptionally regulated.

4.3.2 OGD and AJs

VE-cadherin is the major transmembrane protein of endothelial adhesion junctions. Not only does it mediate the primary contact between two cells, but AJs also influence TJ formation and integrity. Increased VE-cadherin expression has a protective effect on the BBB [99]. Tjap1 KD was differentially expressed in the two cell lines. In cerebEND, Tjap1 KD caused an increase in VE-cadherin expression at both mRNA and protein levels, but the two groups were not statistically significant compared to the normal group. In contrast, in cEND cells, Tjap1 KD caused a decrease in VE-cadherin expression at the mRNA level but an increase at the protein level (Figure 14). This difference may correlate with the cellular origin and the transcriptional process of the protein, but we have not study it. In addition, studies have shown that OGD/R can induce high permeability of endothelial cell monolayers by mediating VE-cadherin internalization [101].

4.3.3 OGD and Inflammatory response

Emerging research suggests that neuroinflammation affects BBB integrity as a risk factor and that the production of multiple cytokines, including Il-1, TNF-α, is primarily responsible for BBB disruption [102]. In the OGD environment, the endothelial cell induce a local inflammatory response and the secretion of pro-inflammatory regulators through upregulation of cell adhesion molecules such as Icam-1 and Vcam-1[53]. Inflammatory mediators released during ischemic brain injury also induce phosphorylation of TJ proteins, resulting in high BBB permeability. We examined the expression of Ccl-2 and -5 and Csf-3 at the mRNA level. Tjap1 KD reduced the expression of the corresponding inflammatory factors, while OGD treatment resulted in an increase in the expression of the inflammatory factors.

This indicates that while OGD can enhance the inflammatory response of cells, Tjap1 KD inhibits this response of cells. In addition, it has been reported that ABC transporter protein expression and their activity can be affected by pro-inflammatory cytokines, resulting in a dose-dependent decrease in P-gp activity and a concomitant decrease in Abcb1 mRNA levels in EC similar to our results [103].

4.3.4 OGD and ABC transporter

ATP-binding cassette proteins (ABC-transporter), which represent an essential class of membrane pumps that actively pump out molecules from cells [104-106], are highly expressed at the BBB. P-gp, also known as multidrug resistance protein 1 (Mdr1 or Abcb1), breast cancer resistance protein (Bcrp or Abcg2), and multidrug resistance-associated proteins (Mrps) are the three primary ABC-transporters at the BBB [107-109]. The transporter P-gp was induced in a model of focal cerebral ischemia in mice and rats [107, 110], consistent with *in vitro* studies showing that OGD treatment regulates P-gp at the mRNA and protein levels [66, 110]. Tjap1 KD in cEND cells caused a statistically significant decrease in P-gp expression at both mRNA and protein levels with no difference due to OGD. The exact mechanism of this Tjap1-mediated regulation is not yet clear.

In parallel, we also examined Mrp1 expression at the mRNA level. Tjap1 KD in cEND cells resulted in a significantly reduced Mrp1 expression with no OGD effect. A previous study showed that Mrp1 levels were slightly reduced in response to focal cerebral ischemia. In isolated brain microvascular fractions, Mrp1 protein expression decreased 3 hours after stroke and partially recovered after 24 - 72 hours [111]. However, in human neocortex after traumatic brain injury, Mrp1 expression was increased in cerebral microvasculature [112]. Therefore, Mrp1 appears to be involved in the hypoxic response of endothelial cells and it expression depends on the Tjap1 protein level.

4.3.5 OGD and ECM

After neurological diseases such as stroke, the BBB and the ECM are simultaneously destroyed, leading to aninflux of solutes, plasma and leukocytes into the brain parenchyma [113, 114]. The main mediator of these processes are the matrix metalloproteinases (Mmps). Mmps are inhibited by Timp and Timp-3 is one of the main regulators [115]. Upregulated Mmps can degrade basement membrane ECM and digest TJ proteins, resulting in BBB leakage [52, 116]. In contrast, disturbed Mmp/Timp-3 homeostasis is associated with BBB dysfunction [117]. In endothelial cells, occludin is hydrolyzed to inactive fragments mostly by Mmp-2/-9 and to a lesser extent by Mmp-3 proteins, leading to barrier disruption [118]. In our experiments, Timp-3 mRNA

expression was significantly reduced in both cEND and cerebEND Tjap1 KD cell lines with no OGD effect. This correlated with the impaired barrier properties of Tjap1 KD cell lines.

4.4 Conclusion

Tjap1 plays an important role in maintaining stable BBB function in endothelial cells and its knock-down causes multiple changes in endothelial phenotype. Tjap1 KD resulted in impaired barrier properties of the endothelial cells as shown by lower TEER values and higher paracellular permeability. Tjap1 KD cell lines proliferated slower but migrated faster in a wound healing assay and showed significantly lower angiogenic capacity in the tube formation assay. These phenotypic changes were accompanied by changes in mRNA and protein expression of TJ and AJ proteins, transporter proteins and inflammatory mediators. Tjap1 expression is regulated in response to OGD and Tjap1 KD resulted in additional damage to the BBB barrier properties under OGD conditions. However, most likely due to cell recovery during the two hour reoxygenation period, no other significant differences were observed between normal and OGD treatment groups. The broad involvement of Tjap1 in the endothelial cell phenotype demonstrated in this work warrants further investigation of its role in brain disorders such as stroke or traumatic brain injury and should be considered in future therapy development strategies.

5. Abstract

Stroke is one of the leading causes of mortality and disability worldwide. The blood-brain barrier (BBB) plays an important role in maintaining brain homeostasis by tightly regulating the exchange of substances between circulating blood and brain parenchyma. BBB disruption is a common pathologic feature of stroke and traumatic brain injury. Understanding the cellular and molecular events that affect the BBB after ischaemic brain injury is important to improve patient prognosis.

We have previously shown that microRNA-212/132 is elevated in hypoxic brain microvascular endothelial cells and acts through suppressing the expression of direct microRNA-212/132 target genes with function at the BBB: claudin-1, junctional adhesion molecule 3 (Jam3) and tight-junction associated protein 1 (Tjap1). While the role of claudin-1 and Jam3 at the BBB is well known, the role of Tjap1 is still unclear. The aim of this work was therefore to characterize the role of Tjap1 in brain endothelial cells using a knock-down (KD) approach in established murine *in vitro* BBB models cEND and cerebEND. Tjap1 KD was established by stable transfection of a plasmid expressing shRNA against Tjap1. The successful downregulation of Tjap1 mRNA and protein was demonstrated by qPCR and Western blot. Tjap1 KD resulted in impaired barrier properties of endothelial cells as shown by lower TEER values and higher paracellular permeability. Interestingly, the Tjap1 KD cells showed lower cell viability and proliferation but migrated faster in a wound healing assay. In the tube formation assay, Tjap1 KD cell lines showed a lower angiogenic potential due to a significantly lower tube length and number as well as a lower amount of branching points in formed capillaries. Tjap1 KD cells showed changes in gene and protein expression. The TJ proteins claudin-5, Jam3 and ZO-1 were significantly increased in Tjap1 KD cell lines, while occludin was strongly decreased. In addition, efflux pump P-glycoprotein was downregulated in Tjap1 KD cells. Oxygen-glucose deprivation (OGD) is a method to mimic stroke *in vitro*. Brain endothelial cell lines treated with OGD showed lower barrier properties compared to cells cultured under normal condition. These effects were more severe in Tjap1 KD cells, indicating active Tjap1 involvement in the OGD response in brain microvascular endothelial cells.

We thus have shown that Tjap1 contributes to a tight barrier of the BBB, regulates cell viability and proliferation of endothelial cells, suppresses their migration and promotes new vessel formation. This means that Tjap1 function is important for mature BBB structure in health and disease.

Zusammenfassung

Schlaganfall ist weltweit eine der häufigsten Ursachen für Mortalität und Behinderung. Die Blut-Hirn-Schranke (BHS) spielt eine wichtige Rolle bei der Aufrechterhaltung der Gehirnhomöostase, indem sie den Stoffaustausch zwischen dem zirkulierenden Blut und dem Gehirnparenchym streng reguliert. Eine Störung der BHS ist ein gemeinsames pathologisches Merkmal von Schlaganfällen und traumatischen Hirnverletzungen. Um die Prognose der Patientinnen und Patienten zu verbessern, ist es wichtig, die zellulären und molekularen Ereignisse zu verstehen, die sich nach einer ischämischen Hirnverletzung auf die BHS auswirken.

Wir haben zuvor gezeigt, dass microRNA-212/132 in hypoxischen mikrovaskulären Endothelzellen erhöht ist und durch die Unterdrückung der Expression direkter Zielgene mit Funktion and der BHS wirkt. Zu den Zielgenen von microRNA-212/132 gehören: Claudin-1, Junctional Adhesion Molecule 3 (Jam3) und Tight Junction Associated Protein 1 (Tjap1). Während die Rolle von Caludin-1 und Jam3 and der BHS gut bekannt ist, ist die Rolle von Tjap1 noch unklar. Ziel dieser Arbeit war es daher, die Rolle von Tjap1 in Endothelzellen mithilfe eines Knock-down (KD)-Ansatzes in etablierten murinen In-vitro-BHS-Modellen zu charakterisieren. Tjap1-KD wurde durch stabile Transfektion eines Plasmids etabliert, das shRNA gegen Tjap1 exprimiert. Die erfolgreiche Herunterregulierung von Tjap1-mRNA und -Protein wurde durch qPCR und Western Blot nachgewiesen. Tjap1-KD führte zu einer Beeinträchtigung der Barriereeigenschaften von Endothelzellen, was sich in niedrigeren TEER-Werten und einer höheren parazellulären Permeabilität wiederspiegelte. Interessanterweise zeigten die Tjap1-KD-Zellen in einem Wundheilungstest eine geringere Zelllebensfähigkeit und Proliferation, wanderten jedoch schneller. Im *tube formation assay* zeigten Tjap1-KD-

Zelllinien ein geringeres Angiogenese-Potential durch eine signifikant geringere Anzahl der gebildeten Kapillaren. Tjap-1-KD-Zellen zeigten Veränderungen in der Gen- und Proteinexpression. Die TJ-Proteinen Claudin-5, Jam3 und ZO-1 waren in Tjap1-KD-Zelllinien signifikant erhöht, während Occludin stark verringert war. Darüber hinaus wurde P-Glykoprotein in Tjap1-KD-Zellen herunterreguliert. Sauerstoff-Glukose-Entzug (eng. *oxygen/glucose-deprivation*, OGD) ist eine Methode zur Nachahmung eines Schlaganfall *in vitro*. Mit OGD behandelte Endothelzelllinien zeigten im Vergleich zu unter normalen Bedingungen kultivierten Zellen geringere Barriereeigenschaften. Diese Effekte waren in Tjap1-KD-Zellen schwerwiegender, was auf eine aktive Beteiligung von Tjap1 an der OGD-Antwort in Endothelzellen hinweist.
Wir haben gezeigt, dass Tjap1 zu einer dichten Barriere der BHS beiträgt, die Zellviabilität und die Proliferation von Endothelzellen reguliert, deren Migration unterdrückt und die Bildung neuer Gefäße fördert. Dies bedeutet, dass die Tjap1-Funktion für die reife BHS-Struktur unter physiologischen und pathophysiologischen Bedingungen wichtig ist.

6. References

1. Campbell BCV, Khatri P: **Stroke**. *Lancet* 2020, **396**(10244):129-142.
2. Zille M, Farr TD, Keep RF, Romer C, Xi G, Boltze J: **Novel targets, treatments, and advanced models for intracerebral haemorrhage**. *EBioMedicine* 2022, **76**:103880.
3. Bowman H, Bonkhoff A, Hope T, Grefkes C, Price C: **Inflated Estimates of Proportional Recovery From Stroke: The Dangers of Mathematical Coupling and Compression to Ceiling**. *Stroke* 2021, **52**(5):1915-1920.
4. Shehjar F, Maktabi B, Rahman ZA, Bahader GA, James AW, Naqvi A, Mahajan R, Shah ZA: **Stroke: Molecular mechanisms and therapies: Update on recent developments**. *Neurochem Int* 2023, **162**:105458.
5. Shi K, Tian DC, Li ZG, Ducruet AF, Lawton MT, Shi FD: **Global brain inflammation in stroke**. *Lancet Neurol* 2019, **18**(11):1058-1066.
6. Yang M, He Y, Deng S, Xiao L, Tian M, Xin Y, Lu C, Zhao F, Gong Y: **Mitochondrial Quality Control: A Pathophysiological Mechanism and Therapeutic Target for Stroke**. *Front Mol Neurosci* 2021, **14**:786099.
7. Li W, Cao F, Takase H, Arai K, Lo EH, Lok J: **Blood-Brain Barrier Mechanisms in Stroke and Trauma**. *Handb Exp Pharmacol* 2022, **273**:267-293.
8. Abbott NJ, Patabendige AA, Dolman DE, Yusof SR, Begley DJ: **Structure and function of the blood-brain barrier**. *Neurobiol Dis* 2010, **37**(1):13-25.
9. Shi H, Liu KJ: **Cerebral tissue oxygenation and oxidative brain injury during ischemia and reperfusion**. *Front Biosci* 2007, **12**:1318-1328.
10. Jiang X, Andjelkovic AV, Zhu L, Yang T, Bennett MVL, Chen J, Keep RF, Shi Y: **Blood-brain barrier dysfunction and recovery after ischemic stroke**. *Prog Neurobiol* 2018, **163-164**:144-171.
11. Blanchette M, Daneman R: **Formation and maintenance of the BBB**. *Mech Dev* 2015, **138 Pt 1**:8-16.
12. Brzica H, Abdullahi W, Ibbotson K, Ronaldson PT: **Role of Transporters in Central Nervous System Drug Delivery and Blood-Brain Barrier Protection: Relevance to Treatment of Stroke**. *J Cent Nerv Syst Dis* 2017, **9**:1179573517693802.
13. Kalogeris T, Baines CP, Krenz M, Korthuis RJ: **Cell biology of ischemia/reperfusion injury**. *Int Rev Cell Mol Biol* 2012, **298**:229-317.
14. Kaupp V, Blecharz-Lang KG, Dilling C, Meybohm P, Burek M: **Protocadherin gamma C3: a new player in regulating vascular barrier function**. *Neural Regen Res* 2023, **18**(1):68-73.
15. Sun A B-LK, Małecki A, Meybohm P, Nowacka-Chmielewska MM, Burek M: **Role of microRNAs in the regulation of blood-brain barrier function in ischemic stroke and under hypoxic conditions in vitro**. *Frontiers in Drug Delivery* 2022, **2-2022**.
16. Scalise AA, Kakogiannos N, Zanardi F, Iannelli F, Giannotta M: **The blood-brain and gut-vascular barriers: from the perspective of claudins**. *Tissue Barriers* 2021, **9**(3):1926190.
17. Butt AM, Jones HC, Abbott NJ: **Electrical resistance across the blood-brain barrier in anaesthetized rats: a developmental study**. *J Physiol* 1990, **429**:47-62.
18. Ronaldson PT, Davis TP: **Targeting transporters: promoting blood-brain barrier repair in response to oxidative stress injury**. *Brain Res* 2015, **1623**:39-52.

19. Kaisar MA, Sajja RK, Prasad S, Abhyankar VV, Liles T, Cucullo L: **New experimental models of the blood-brain barrier for CNS drug discovery**. *Expert Opin Drug Discov* 2017, **12**(1):89-103.
20. Berndt P, Winkler L, Cording J, Breitkreuz-Korff O, Rex A, Dithmer S, Rausch V, Blasig R, Richter M, Sporbert A *et al*: **Tight junction proteins at the blood-brain barrier: far more than claudin-5**. *Cell Mol Life Sci* 2019, **76**(10):1987-2002.
21. Dithmer S, Staat C, Muller C, Ku MC, Pohlmann A, Niendorf T, Gehne N, Fallier-Becker P, Kittel A, Walter FR *et al*: **Claudin peptidomimetics modulate tissue barriers for enhanced drug delivery**. *Ann N Y Acad Sci* 2017, **1397**(1):169-184.
22. Haseloff RF, Dithmer S, Winkler L, Wolburg H, Blasig IE: **Transmembrane proteins of the tight junctions at the blood-brain barrier: structural and functional aspects**. *Semin Cell Dev Biol* 2015, **38**:16-25.
23. Reinhold AK, Rittner HL: **Barrier function in the peripheral and central nervous system-a review**. *Pflugers Arch* 2017, **469**(1):123-134.
24. Sladojevic N, Stamatovic SM, Keep RF, Grailer JJ, Sarma JV, Ward PA, Andjelkovic AV: **Inhibition of junctional adhesion molecule-A/LFA interaction attenuates leukocyte trafficking and inflammation in brain ischemia/reperfusion injury**. *Neurobiol Dis* 2014, **67**:57-70.
25. Williams DW, Calderon TM, Lopez L, Carvallo-Torres L, Gaskill PJ, Eugenin EA, Morgello S, Berman JW: **Mechanisms of HIV entry into the CNS: increased sensitivity of HIV infected CD14+CD16+ monocytes to CCL2 and key roles of CCR2, JAM-A, and ALCAM in diapedesis**. *PLoS One* 2013, **8**(7):e69270.
26. Furuse M, Fujita K, Hiiragi T, Fujimoto K, Tsukita S: **Claudin-1 and -2: novel integral membrane proteins localizing at tight junctions with no sequence similarity to occludin**. *J Cell Biol* 1998, **141**(7):1539-1550.
27. Lal-Nag M, Morin PJ: **The claudins**. *Genome Biol* 2009, **10**(8):235.
28. Abbruscato TJ, Lopez SP, Mark KS, Hawkins BT, Davis TP: **Nicotine and cotinine modulate cerebral microvascular permeability and protein expression of ZO-1 through nicotinic acetylcholine receptors expressed on brain endothelial cells**. *J Pharm Sci* 2002, **91**(12):2525-2538.
29. Fischer S, Wobben M, Marti HH, Renz D, Schaper W: **Hypoxia-induced hyperpermeability in brain microvessel endothelial cells involves VEGF-mediated changes in the expression of zonula occludens-1**. *Microvasc Res* 2002, **63**(1):70-80.
30. Mark KS, Davis TP: **Cerebral microvascular changes in permeability and tight junctions induced by hypoxia-reoxygenation**. *Am J Physiol Heart Circ Physiol* 2002, **282**(4):H1485-1494.
31. Fanning AS, Jameson BJ, Jesaitis LA, Anderson JM: **The tight junction protein ZO-1 establishes a link between the transmembrane protein occludin and the actin cytoskeleton**. *J Biol Chem* 1998, **273**(45):29745-29753.
32. Wevers NR, de Vries HE: **Morphogens and blood-brain barrier function in health and disease**. *Tissue Barriers* 2016, **4**(1):e1090524.
33. Kawabe H, Nakanishi H, Asada M, Fukuhara A, Morimoto K, Takeuchi M, Takai Y: **Pilt, a novel peripheral membrane protein at tight junctions in epithelial cells**. *J Biol Chem* 2001, **276**(51):48350-48355.
34. Tamaki H, Sanda M, Katsumata O, Hara Y, Fukaya M, Sakagami H: **Pilt is a coiled-coil domain-containing protein that localizes at the trans-Golgi complex and regulates its structure**. *FEBS Lett* 2012, **586**(19):3064-3070.

35. Tariq H, Bella J, Jowitt TA, Holmes DF, Rouhi M, Nie Z, Baldock C, Garrod D, Tabernero L: **Cadherin flexibility provides a key difference between desmosomes and adherens junctions**. *Proc Natl Acad Sci U S A* 2015, **112**(17):5395-5400.
36. Hartsock A, Nelson WJ: **Adherens and tight junctions: structure, function and connections to the actin cytoskeleton**. *Biochim Biophys Acta* 2008, **1778**(3):660-669.
37. Abdullahi W, Tripathi D, Ronaldson PT: **Blood-brain barrier dysfunction in ischemic stroke: targeting tight junctions and transporters for vascular protection**. *Am J Physiol Cell Physiol* 2018, **315**(3):C343-C356.
38. Luissint AC, Artus C, Glacial F, Ganeshamoorthy K, Couraud PO: **Tight junctions at the blood brain barrier: physiological architecture and disease-associated dysregulation**. *Fluids Barriers CNS* 2012, **9**(1):23.
39. Redzic Z: **Molecular biology of the blood-brain and the blood-cerebrospinal fluid barriers: similarities and differences**. *Fluids Barriers CNS* 2011, **8**(1):3.
40. Hashimoto Y, Campbell M: **Tight junction modulation at the blood-brain barrier: Current and future perspectives**. *Biochim Biophys Acta Biomembr* 2020, **1862**(9):183298.
41. Bayir E, Sendemir A: **Role of Intermediate Filaments in Blood-Brain Barrier in Health and Disease**. *Cells* 2021, **10**(6).
42. Takai Y, Miyoshi J, Ikeda W, Ogita H: **Nectins and nectin-like molecules: roles in contact inhibition of cell movement and proliferation**. *Nat Rev Mol Cell Biol* 2008, **9**(8):603-615.
43. Takai Y, Ikeda W, Ogita H, Rikitake Y: **The immunoglobulin-like cell adhesion molecule nectin and its associated protein afadin**. *Annu Rev Cell Dev Biol* 2008, **24**:309-342.
44. Takai Y, Nakanishi H: **Nectin and afadin: novel organizers of intercellular junctions**. *J Cell Sci* 2003, **116**(Pt 1):17-27.
45. Mohi-Ud-Din R, Mir RH, Mir PA, Banday N, Shah AJ, Sawhney G, Bhat MM, Batiha GE, Pottoo FH: **Dysfunction of ABC Transporters at the Surface of BBB: Potential Implications in Intractable Epilepsy and Applications of Nanotechnology Enabled Drug Delivery**. *Curr Drug Metab* 2022, **23**(9):735-756.
46. Tome ME, Herndon JM, Schaefer CP, Jacobs LM, Zhang Y, Jarvis CK, Davis TP: **P-glycoprotein traffics from the nucleus to the plasma membrane in rat brain endothelium during inflammatory pain**. *J Cereb Blood Flow Metab* 2016, **36**(11):1913-1928.
47. Abdullahi W, Davis TP, Ronaldson PT: **Functional Expression of P-glycoprotein and Organic Anion Transporting Polypeptides at the Blood-Brain Barrier: Understanding Transport Mechanisms for Improved CNS Drug Delivery?** *AAPS J* 2017, **19**(4):931-939.
48. Hennessy M, Spiers JP: **A primer on the mechanics of P-glycoprotein the multidrug transporter**. *Pharmacol Res* 2007, **55**(1):1-15.
49. Kammeijer GSM, Nouta J, de la Rosette J, de Reijke TM, Wuhrer M: **An In-Depth Glycosylation Assay for Urinary Prostate-Specific Antigen**. *Anal Chem* 2018, **90**(7):4414-4421.
50. Hanssen KM, Haber M, Fletcher JI: **Targeting multidrug resistance-associated protein 1 (MRP1)-expressing cancers: Beyond pharmacological inhibition**. *Drug Resist Updat* 2021, **59**:100795.
51. Smolarz B, Makowska M, Romanowicz H: **Pharmacogenetics of Drug-Resistant Epilepsy (Review of Literature)**. *Int J Mol Sci* 2021, **22**(21).

52. Zhao Y, Gan L, Ren L, Lin Y, Ma C, Lin X: **Factors influencing the blood-brain barrier permeability**. *Brain Res* 2022, **1788**:147937.
53. Zhou Y, Khan H, Hoi MPM, Cheang WS: **Piceatannol Protects Brain Endothelial Cell Line (bEnd.3) against Lipopolysaccharide-Induced Inflammation and Oxidative Stress**. *Molecules* 2022, **27**(4).
54. Ittner C, Burek M, Stork S, Nagai M, Forster CY: **Increased Catecholamine Levels and Inflammatory Mediators Alter Barrier Properties of Brain Microvascular Endothelial Cells in vitro**. *Front Cardiovasc Med* 2020, **7**:73.
55. Rochfort KD, Cummins PM: **The blood-brain barrier endothelium: a target for pro-inflammatory cytokines**. *Biochem Soc Trans* 2015, **43**(4):702-706.
56. Salvador E, Burek M, Forster CY: **Stretch and/or oxygen glucose deprivation (OGD) in an in vitro traumatic brain injury (TBI) model induces calcium alteration and inflammatory cascade**. *Front Cell Neurosci* 2015, **9**:323.
57. Persidsky Y, Ramirez SH, Haorah J, Kanmogne GD: **Blood-brain barrier: structural components and function under physiologic and pathologic conditions**. *J Neuroimmune Pharmacol* 2006, **1**(3):223-236.
58. Stamatovic SM, Johnson AM, Sladojevic N, Keep RF, Andjelkovic AV: **Endocytosis of tight junction proteins and the regulation of degradation and recycling**. *Ann N Y Acad Sci* 2017, **1397**(1):54-65.
59. Klein T, Bischoff R: **Physiology and pathophysiology of matrix metalloproteases**. *Amino Acids* 2011, **41**(2):271-290.
60. Li W, Chen Z, Yuan J, Yu Z, Cheng C, Zhao Q, Huang L, Hajjar KA, Chen Z, Lo EH *et al*: **Annexin A2 is a Robo4 ligand that modulates ARF6 activation-associated cerebral trans-endothelial permeability**. *J Cereb Blood Flow Metab* 2019, **39**(10):2048-2060.
61. Rosenberg GA, Kornfeld M, Estrada E, Kelley RO, Liotta LA, Stetler-Stevenson WG: **TIMP-2 reduces proteolytic opening of blood-brain barrier by type IV collagenase**. *Brain Res* 1992, **576**(2):203-207.
62. Abdul-Muneer PM, Pfister BJ, Haorah J, Chandra N: **Role of Matrix Metalloproteinases in the Pathogenesis of Traumatic Brain Injury**. *Mol Neurobiol* 2016, **53**(9):6106-6123.
63. Abdul-Muneer PM, Schuetz H, Wang F, Skotak M, Jones J, Gorantla S, Zimmerman MC, Chandra N, Haorah J: **Induction of oxidative and nitrosative damage leads to cerebrovascular inflammation in an animal model of mild traumatic brain injury induced by primary blast**. *Free Radic Biol Med* 2013, **60**:282-291.
64. Petty MA, Lo EH: **Junctional complexes of the blood-brain barrier: permeability changes in neuroinflammation**. *Prog Neurobiol* 2002, **68**(5):311-323.
65. Witt KA, Mark KS, Sandoval KE, Davis TP: **Reoxygenation stress on blood-brain barrier paracellular permeability and edema in the rat**. *Microvasc Res* 2008, **75**(1):91-96.
66. Neuhaus W, Gaiser F, Mahringer A, Franz J, Riethmuller C, Forster C: **The pivotal role of astrocytes in an in vitro stroke model of the blood-brain barrier**. *Front Cell Neurosci* 2014, **8**:352.
67. Silwedel C, Forster C: **Differential susceptibility of cerebral and cerebellar murine brain microvascular endothelial cells to loss of barrier properties in response to inflammatory stimuli**. *J Neuroimmunol* 2006, **179**(1-2):37-45.
68. Forster C, Silwedel C, Golenhofen N, Burek M, Kietz S, Mankertz J, Drenckhahn D: **Occludin as direct target for glucocorticoid-induced improvement of blood-brain barrier properties in a murine in vitro system**. *J Physiol* 2005, **565**(Pt 2):475-486.

69. Blecharz KG, Drenckhahn D, Forster CY: **Glucocorticoids increase VE-cadherin expression and cause cytoskeletal rearrangements in murine brain endothelial cEND cells**. *J Cereb Blood Flow Metab* 2008, **28**(6):1139-1149.
70. Burek M, Forster CY: **Cloning and characterization of the murine claudin-5 promoter**. *Mol Cell Endocrinol* 2009, **298**(1-2):19-24.
71. Harke N, Leers J, Kietz S, Drenckhahn D, Forster C: **Glucocorticoids regulate the human occludin gene through a single imperfect palindromic glucocorticoid response element**. *Mol Cell Endocrinol* 2008, **295**(1-2):39-47.
72. Reschke M, Salvador E, Schlegel N, Burek M, Karnati S, Wunder C, Forster CY: **Isosteviol Sodium (STVNA) Reduces Pro-Inflammatory Cytokine IL-6 and GM-CSF in an In Vitro Murine Stroke Model of the Blood-Brain Barrier (BBB)**. *Pharmaceutics* 2022, **14**(9).
73. Rosing N, Salvador E, Guntzel P, Kempe C, Burek M, Holzgrabe U, Soukhoroukov V, Wunder C, Forster C: **Neuroprotective Effects of Isosteviol Sodium in Murine Brain Capillary Cerebellar Endothelial Cells (cerebEND) After Hypoxia**. *Front Cell Neurosci* 2020, **14**:573950.
74. Gabbert L, Dilling C, Meybohm P, Burek M: **Deletion of Protocadherin Gamma C3 Induces Phenotypic and Functional Changes in Brain Microvascular Endothelial Cells In Vitro**. *Front Pharmacol* 2020, **11**:590144.
75. Burek M, Burmester S, Salvador E, Moller-Ehrlich K, Schneider R, Roewer N, Nagai M, Forster CY: **Kidney Ischemia/Reperfusion Injury Induces Changes in the Drug Transporter Expression at the Blood-Brain Barrier in vivo and in vitro**. *Front Physiol* 2020, **11**:569881.
76. Gerhartl A, Hahn K, Neuhoff A, Friedl HP, Forster CY, Wunder C, Schick M, Burek M, Neuhaus W: **Hydroxyethylstarch (130/0.4) tightens the blood-brain barrier in vitro**. *Brain Res* 2020, **1727**:146560.
77. Kaiser M, Burek M, Britz S, Lankamp F, Ketelhut S, Kemper B, Forster C, Gorzelanny C, Goycoolea FM: **The Influence of Capsaicin on the Integrity of Microvascular Endothelial Cell Monolayers**. *Int J Mol Sci* 2018, **20**(1).
78. Salvador E, Burek M, Lohr M, Nagai M, Hagemann C, Forster CY: **Senescence and associated blood-brain barrier alterations in vitro**. *Histochem Cell Biol* 2021, **156**(3):283-292.
79. Burek M HA, Gold R, Roewer N, Chan A, Förster CY: **Differential cytokine release from brain microvascular endothelial cells treated with dexamethasone and multiple sclerosis patient sera**. *J of Steroids & Hormonal Science* 2014, **5:128**.
80. Burek M, Konig A, Lang M, Fiedler J, Oerter S, Roewer N, Bohnert M, Thal SC, Blecharz-Lang KG, Woitzik J *et al*: **Hypoxia-Induced MicroRNA-212/132 Alter Blood-Brain Barrier Integrity Through Inhibition of Tight Junction-Associated Proteins in Human and Mouse Brain Microvascular Endothelial Cells**. *Transl Stroke Res* 2019, **10**(6):672-683.
81. Burek M, Salvador E, Forster CY: **Generation of an immortalized murine brain microvascular endothelial cell line as an in vitro blood brain barrier model**. *J Vis Exp* 2012(66):e4022.
82. Towbin H, Staehelin T, Gordon J: **Electrophoretic transfer of proteins from polyacrylamide gels to nitrocellulose sheets: procedure and some applications**. *Proc Natl Acad Sci U S A* 1979, **76**(9):4350-4354.
83. Feldheim J, Wend D, Lauer MJ, Monoranu CM, Glas M, Kleinschnitz C, Ernestus RI, Braunger BM, Meybohm P, Hagemann C *et al*: **Protocadherin Gamma C3 (PCDHGC3) Is Strongly Expressed in Glioblastoma and Its High Expression Is Associated with Longer Progression-Free Survival of Patients**. *Int J Mol Sci* 2022, **23**(15).

84. Blecharz-Lang KG, Prinz V, Burek M, Frey D, Schenkel T, Krug SM, Fromm M, Vajkoczy P: **Gelatinolytic activity of autocrine matrix metalloproteinase-9 leads to endothelial de-arrangement in Moyamoya disease**. *J Cereb Blood Flow Metab* 2018, **38**(11):1940-1953.
85. Stamatovic SM, Johnson AM, Keep RF, Andjelkovic AV: **Junctional proteins of the blood-brain barrier: New insights into function and dysfunction**. *Tissue Barriers* 2016, **4**(1):e1154641.
86. Lambeth LS, Smith CA: **Short hairpin RNA-mediated gene silencing**. *Methods Mol Biol* 2013, **942**:205-232.
87. Yan H, Kanki H, Matsumura S, Kawano T, Nishiyama K, Sugiyama S, Takemori H, Mochizuki H, Sasaki T: **MiRNA-132/212 regulates tight junction stabilization in blood-brain barrier after stroke**. *Cell Death Discov* 2021, **7**(1):380.
88. Tsukita S, Tanaka H, Tamura A: **The Claudins: From Tight Junctions to Biological Systems**. *Trends Biochem Sci* 2019, **44**(2):141-152.
89. Yu P, Li Y, Zhong G, Li W, Chen B, Zhang J: **Claudin-5 Affects Endothelial Autophagy in Response to Early Hypoxia**. *Front Physiol* 2021, **12**:737474.
90. Bamforth SD, Kniesel U, Wolburg H, Engelhardt B, Risau W: **A dominant mutant of occludin disrupts tight junction structure and function**. *J Cell Sci* 1999, **112 (Pt 12)**:1879-1888.
91. Du H, Wang S: **Omarigliptin Mitigates Lipopolysaccharide-Induced Neuroinflammation and Dysfunction of the Integrity of the Blood-Brain Barrier**. *ACS Chem Neurosci* 2020, **11**(24):4262-4269.
92. Nitta T, Hata M, Gotoh S, Seo Y, Sasaki H, Hashimoto N, Furuse M, Tsukita S: **Size-selective loosening of the blood-brain barrier in claudin-5-deficient mice**. *J Cell Biol* 2003, **161**(3):653-660.
93. Piontek J, Fritzsche S, Cording J, Richter S, Hartwig J, Walter M, Yu D, Turner JR, Gehring C, Rahn HP *et al*: **Elucidating the principles of the molecular organization of heteropolymeric tight junction strands**. *Cell Mol Life Sci* 2011, **68**(23):3903-3918.
94. Coyne CB, Gambling TM, Boucher RC, Carson JL, Johnson LG: **Role of claudin interactions in airway tight junctional permeability**. *Am J Physiol Lung Cell Mol Physiol* 2003, **285**(5):L1166-1178.
95. Tornabene E, Helms HCC, Pedersen SF, Brodin B: **Effects of oxygen-glucose deprivation (OGD) on barrier properties and mRNA transcript levels of selected marker proteins in brain endothelial cells/astrocyte co-cultures**. *PLoS One* 2019, **14**(8):e0221103.
96. Castro Dias M, Coisne C, Baden P, Enzmann G, Garrett L, Becker L, Holter SM, German Mouse Clinic C, Hrabe de Angelis M, Deutsch U *et al*: **Claudin-12 is not required for blood-brain barrier tight junction function**. *Fluids Barriers CNS* 2019, **16**(1):30.
97. Ebnet K: **Junctional Adhesion Molecules (JAMs): Cell Adhesion Receptors With Pleiotropic Functions in Cell Physiology and Development**. *Physiol Rev* 2017, **97**(4):1529-1554.
98. Keiper T, Santoso S, Nawroth PP, Orlova V, Chavakis T: **The role of junctional adhesion molecules in cell-cell interactions**. *Histol Histopathol* 2005, **20**(1):197-203.
99. Zeng X, He G, Yang X, Xu G, Tang Y, Li H, Yu B, Wang Z, Xu W, Song K: **Zebularine protects against blood-brain-barrier (BBB) disruption through increasing the expression of zona occludens-1 (ZO-1) and vascular endothelial (VE)-cadherin**. *Bioengineered* 2022, **13**(2):4441-4454.
100. Sun K, Fan J, Han J: **Ameliorating effects of traditional Chinese medicine preparation, Chinese materia medica and active compounds on**

ischemia/reperfusion-induced cerebral microcirculatory disturbances and neuron damage. *Acta Pharm Sin B* 2015, **5**(1):8-24.

101. Chen J, Sun L, Ding GB, Chen L, Jiang L, Wang J, Wu J: **Oxygen-Glucose Deprivation/Reoxygenation Induces Human Brain Microvascular Endothelial Cell Hyperpermeability Via VE-Cadherin Internalization: Roles of RhoA/ROCK2**. *J Mol Neurosci* 2019, **69**(1):49-59.
102. Kvichansky AA, Volobueva MN, Spivak YS, Tret'yakova LV, Gulyaeva NV, Bolshakov AP: **Expression of mRNAs for IL-1beta, IL-6, IL-10, TNFalpha, CX3CL1, and TGFbeta1 Cytokines in the Brain Tissues: Assessment of Contribution of Blood Cells with and without Perfusion**. *Biochemistry (Mosc)* 2019, **84**(8):905-910.
103. Iqbal M, Ho HL, Petropoulos S, Moisiadis VG, Gibb W, Matthews SG: **Pro-inflammatory cytokine regulation of P-glycoprotein in the developing blood-brain barrier**. *PLoS One* 2012, **7**(8):e43022.
104. Helms HC, Abbott NJ, Burek M, Cecchelli R, Couraud PO, Deli MA, Forster C, Galla HJ, Romero IA, Shusta EV *et al*: **In vitro models of the blood-brain barrier: An overview of commonly used brain endothelial cell culture models and guidelines for their use**. *J Cereb Blood Flow Metab* 2016, **36**(5):862-890.
105. Tornabene E, Brodin B: **Stroke and Drug Delivery--In Vitro Models of the Ischemic Blood-Brain Barrier**. *J Pharm Sci* 2016, **105**(2):398-405.
106. Verscheijden LFM, van Hattem AC, Pertijs J, de Jongh CA, Verdijk RM, Smeets B, Koenderink JB, Russel FGM, de Wildt SN: **Developmental patterns in human blood-brain barrier and blood-cerebrospinal fluid barrier ABC drug transporter expression**. *Histochem Cell Biol* 2020, **154**(3):265-273.
107. Miller DS: **Regulation of ABC transporters at the blood-brain barrier**. *Clin Pharmacol Ther* 2015, **97**(4):395-403.
108. Behl T, Kaur I, Sehgal A, Kumar A, Uddin MS, Bungau S: **The Interplay of ABC Transporters in Abeta Translocation and Cholesterol Metabolism: Implicating Their Roles in Alzheimer's Disease**. *Mol Neurobiol* 2021, **58**(4):1564-1582.
109. de Gooijer MC, Kemper EM, Buil LCM, Citirikkaya CH, Buckle T, Beijnen JH, van Tellingen O: **ATP-binding cassette transporters restrict drug delivery and efficacy against brain tumors even when blood-brain barrier integrity is lost**. *Cell Rep Med* 2021, **2**(1):100184.
110. DeMars KM, Yang C, Hawkins KE, McCrea AO, Siwarski DM, Candelario-Jalil E: **Spatiotemporal Changes in P-glycoprotein Levels in Brain and Peripheral Tissues Following Ischemic Stroke in Rats**. *J Exp Neurosci* 2017, **11**:1179069517701741.
111. Kilic E, Spudich A, Kilic U, Rentsch KM, Vig R, Matter CM, Wunderli-Allenspach H, Fritschy JM, Bassetti CL, Hermann DM: **ABCC1: a gateway for pharmacological compounds to the ischaemic brain**. *Brain* 2008, **131**(Pt 10):2679-2689.
112. Willyerd FA, Empey PE, Philbrick A, Ikonomovic MD, Puccio AM, Kochanek PM, Okonkwo DO, Clark RS: **Expression of ATP-Binding Cassette Transporters B1 and C1 after Severe Traumatic Brain Injury in Humans**. *J Neurotrauma* 2016, **33**(2):226-231.
113. Haorah J, Ramirez SH, Schall K, Smith D, Pandya R, Persidsky Y: **Oxidative stress activates protein tyrosine kinase and matrix metalloproteinases leading to blood-brain barrier dysfunction**. *J Neurochem* 2007, **101**(2):566-576.

114. Leppert D, Lindberg RL, Kappos L, Leib SL: **Matrix metalloproteinases: multifunctional effectors of inflammation in multiple sclerosis and bacterial meningitis**. *Brain Res Brain Res Rev* 2001, **36**(2-3):249-257.
115. Hartmann C, El-Gindi J, Lohmann C, Lischper M, Zeni P, Galla HJ: **TIMP-3: a novel target for glucocorticoid signaling at the blood-brain barrier**. *Biochem Biophys Res Commun* 2009, **390**(2):182-186.
116. Vafadari B, Salamian A, Kaczmarek L: **MMP-9 in translation: from molecule to brain physiology, pathology, and therapy**. *J Neurochem* 2016, **139 Suppl 2**:91-114.
117. Mi X, Cao Y, Li Y, Li Y, Hong J, He J, Liang Y, Yang N, Liu T, Han D *et al*: **The Non-peptide Angiotensin-(1-7) Mimic AVE 0991 Attenuates Delayed Neurocognitive Recovery After Laparotomy by Reducing Neuroinflammation and Restoring Blood-Brain Barrier Integrity in Aged Rats**. *Front Aging Neurosci* 2021, **13**:624387.
118. Cummins PM: **Occludin: one protein, many forms**. *Mol Cell Biol* 2012, **32**(2):242-250.

Appendix

I. Abbreviations

Ab	Antibody
AP	Action potentials
BBB	Blood brain barrier
CSF	Colony stimulating factor
CCL	Chemokine ligand
ECs	Endothelial cells
FITC	Fluoroscein isothicyanate
KD	Knock-down
PVDF	Polyvinylidene fluoride
SDS-PAGE	Sodium dodecyl sulfate-polyacrylamide gel electrophoresis
TJP	Tight junction protein
WB	Western blot
AJ	Adherens Junction
BSA	Bovines Serumalbumin
DMEM	Dulbeco's modified eagle medium
ECM	Extracellular matrix
JAM	Junctional adhesion molecule
ZO	Zonula occludens
Tjap	Tight junction-associated protein
TEER	Transendothelial Electrical Resistance
VCAM	Vascular cell adhesion molecule
VEGF	Vascular Endothelial Growth Factor
TIMP	Metalloproteinase inhibitor
Pgp	Permeability glycoprotein
µg	Microgram
µm	Micrometer
ml	Milliliter

II. List of figures

III. List of tables

Acknowledgments

I am particularly grateful to PD Dr. rer. nat. Malgorzata Burek, who accepted my application and gave me the opportunity to do my doctoral thesis in her research group. I am also grateful to the Department of Anaesthesiology for being a platform for experimentation. I would like to thank my supervisor for her help and guidance during my experiments, for always being the first person to talk to when I encountered a problem, and for her patience during the writing of my doctoral thesis.

Next, I would like to thank Ms. A. Neuhoff, Ms. E. Wilken and Ms. K. Steinisch. They supported me as laboratory assistants and taught me the basics of laboratory work and skills. They were always there to help me technically and always had unique suggestions for my questions, which helped me a lot with the laboratory process.

I would like to thank the hospital where I am currently working and the leaders who have supported me financially and given me some guidance in my career during my studies. Their help has given me the opportunity to stand here, learn more, experience a different culture and meet more people.

Finally, I would like to thank my friends and family for their persistent support and patience and comfort. Studying for my doctoral degree and writing this thesis in Germany was not easy and I encountered many problems and bad feelings. I thank them for their love and tolerance. This gave me the courage to do this work.

Curriculum vitae

Publications and conference participations

Aili Sun, Kinga G. Blecharz-Lang, Andrzej Malecki, Patrick Meybohm, Marta M. Nowacka-Chmielewska, Malgorzata Burek. Role of microRNAs in the regulation of blood-brain barrier function in ischemic stroke and under hypoxic conditions in vitro. Front. Drug Deliv. 01 November 2022. https://doi.org/10.3389/fddev.2022.1027098

Congress Participations

Aili Sun, Laura Härtel, Patrick Meybohm, Malgorzata Burek (2022). Targets of MicroRNA-212/132 and their role at the Blood-Brain Barrier. 24th International Symposium on Signal Transduction at the Blood-Brain Barriers. September, 21-23 2022, Bari (Italy). Poster.